

Supporting Information for

Fluorescence Detected Circular Dichroism (FDCD) of a Stereodynamic Probe

Authors: Roberto Penasa,^a Federico Begato,^a Giulia Licini,^a Klaus Wurst,^b Sergio Abbate,^c Giovanna Longhi^c
and Cristiano Zonta^{*a}

- a. Dipartimento di Scienze Chimiche, Università degli Studi di Padova, Via Marzolo 1, 35131 - Padova – PD (Italy)
- b. Department of General, Inorganic and Theoretical Chemistry, University of Innsbruck A-6020 Innsbruck, Austria.
- c. Department of Molecular and Translational Medicine, Viale Europa 11 - 25123 Brescia – BS (Italy) and Istituto Nazionale di Ottica (INO), CNR, Research Unit of Brescia, 25123 Brescia, Italy.

*Correspondence to: cristiano.zonta@unipd.it

1. Contents

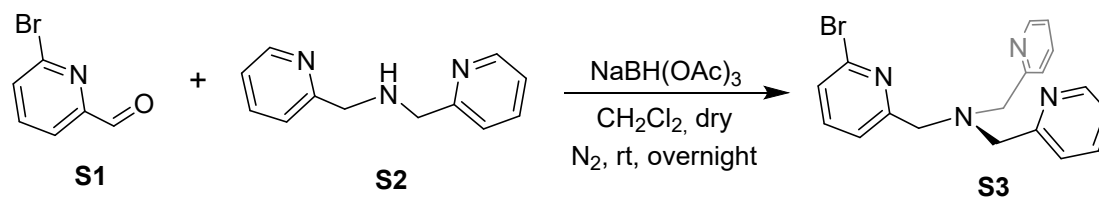
1. Contents	2
2. General Methods	4
3. Synthesis and Characterization	5
3.1 Synthesis of 1-(6-bromopyridin-2-yl)-N,N-bis(pyridin-2-ylmethyl)methanamine S3	5
3.2 Synthesis of 1-(6-(anthracen-1-yl)pyridin-2-yl)-N,N-bis(pyridin-2-ylmethyl)methanamine S5	6
3.3 Synthesis of complex 1	7
4. ¹ H-NMR and ESI-MS characterization	8
5. UV-Vis Measurements	12
5.1 Uv-Vis measurements of complex 1	12
5.2 Uv-Vis titration of complex 1 with <i>R</i> -methoxyphenylacetic acid <i>R</i> -MetMan	13
5.3 Uv-Vis measurements of a selected series of carboxylic acids	14
6. Fluorescence Measurements	15
6.1 Fluorescence titration of complex 1 with <i>R</i> -methoxyphenylacetic acid <i>R</i> -MetMan	16
6.2 Fluorescence measurements of the “chiroptical contaminant” <i>R</i> -BINAPO and complex 1	17
6.3 Fluorescence measurements of the “chiroptical contaminant” (-)-Riboflavin and complex 1	18
7. ECD measurements	19
7.1 ECD titration complex 1 (10 ⁻⁵ M) with <i>R</i> -methoxyphenylacetic acid <i>R</i> -MetMan	19
7.2 ECD titration of complex 1 (2×10 ⁻⁴ M) with <i>S</i> -methoxyphenylacetic acid <i>S</i> -MetMan	20
7.3 ECD sensing capability	21
7.4 ECD measurements of a selected series of carboxylic acids	21
7.5 Enantiomeric excess calibration curve of MetMan acid versus CD amplitude	22
7.6 ECD titration of complex 1 (10 ⁻⁵ M) and <i>R</i> -MetMan (5×10 ⁻⁴ M) acid with <i>R</i> -BINAPO	23
8. FDCD measurements	25
8.1 FDCD titration complex 1 with <i>R</i> -methoxyphenylacetic acid <i>R</i> -MetMan	25
8.2 FDCD sensing capability	26
8.3 FDCD measurements of a selected series of carboxylic acids	26
8.4 Enantiomeric excess calibration curve of MetMan acid versus FDCD amplitude	27
8.5 FDCD titration of complex 1 (10 ⁻⁵ M) and <i>R</i> -MetMan (5×10 ⁻⁴ M) acid with <i>R</i> -BINAPO	28
8.6 FDCD titration of complex 1 (10 ⁻⁵ M) and <i>R</i> -MetMan (5×10 ⁻⁴ M) acid with (-)-Riboflavin	30
9. X-Ray measurements	32
9.1 Refinement Data for the species <i>R</i> -MetMan·1	32
9.2 Coordinates of the Atoms within the Unit Cell	33
10. DFT Calculation	38
11. References	44

2. General Methods

NMR spectra were recorded at 301 K on Bruker Avance DMX 500 MHz or Bruker Avance-300 MHz instruments. All the ^1H -NMR spectra were referenced to residual isotopic impurity of CDCl_3 (7.26 ppm), DMSO-d_6 (2.50 ppm) or CD_3CN (1.94 ppm). The following abbreviations are used in reporting the multiplicity for NMR resonances: s=single, d=doublet, t= triplet, q=quartet, and m=multiplet. The NMR data were processed using Bruker Topspin 3.5 pl2 and MestReNova 12.0.2. ESI-MS spectra have been acquired with an Agilent Technology LC/MSD Trap SL interfaced to an Agilent 1100 binary pump. The samples were previously dissolved in acetonitrile and subsequently directly injected with a solvent flow rate of 0.05 mL/min. MS peak intensity for each analysis is reported as monoisotopic mass and the data were processed with MestReNova 12.0.2. UV-Vis spectra were recorded with a Varian Cary 50 spectrophotometer. Fluorescence spectra were recorded with an Agilent Cary Eclipse spectrophotometer. ECD and FDCD spectra were recorded with a Jasco J-1500 spectrophotometer. The spectra were processed with Spectra Manager Version 2.13.0.0 and OriginPro 2018 (64-bit) SR1 b9.5.1.195. Chemicals were purchased from Aldrich, TCI, or Apollo Scientific and used without further purification.

3. Synthesis and Characterization

3.1 Synthesis of 1-(6-bromopyridin-2-yl)-N,N-bis(pyridin-2-ylmethyl)methanamine S3

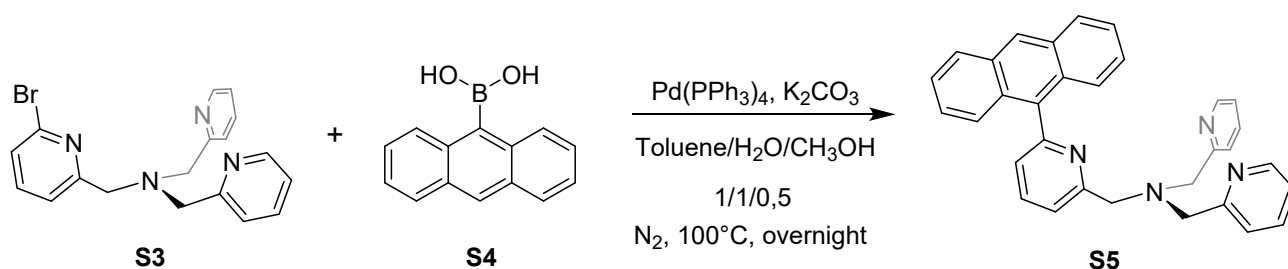


In a Schlenk apparatus, 6-bromopyridine-2-carboxaldehyde **S1** (1.55 g, 8.34 mmol) and di-(2-picolyl)amine (1.5 mL, 8.33 mmol) were dissolved in 15 mL of dry CH₂Cl₂ under N₂. The reaction mixture is left under stirring for one hour. Three aliquots of the reducing agent NaBH(OAc)₃ (0.589, 0.603 and 0.702 g, respectively 2.78, 2.84 and 3.31 mmol) were added waiting 20 minutes between each addition. The reaction mixture is left under stirring overnight at room temperature. The solvent was removed under reduced pressure. The resulting product was dissolved in EtOAc and the solution extracted with 0.1 M solution of KOH (3x50 mL). The organic phases were dried with Na₂SO₄ and the solvent was removed under reduced pressure. The resulting brown oil was precipitated by crystallization from THF/n-hexane, after storing it in the freezer (-20°C), to yield the product as pale-yellow solids (2.16g, 5.65 mmol, 67%).

¹H-NMR (CDCl₃, 300 MHz); δ(ppm): 8.58 – 8.48 (m, 2H), 7.65 (td, J = 7.6, 1.8 Hz, 2H), 7.52 (dt, J = 20.4, 7.4 Hz, 4H), 7.31 (d, J = 7.6 Hz, 1H), 7.19 – 7.09 (m, 2H), 3.88 (d, J = 4.6 Hz, 6H).

ESI-MS (m/z): theoretical mass for [C₃₂H₂₇N₄+H]⁺ = 369.06 m/z ; found = 369.30 m/z.

3.2 Synthesis of 1-(6-(anthracen-1-yl)pyridin-2-yl)-N,N-bis(pyridin-2-yl)methanamine S5



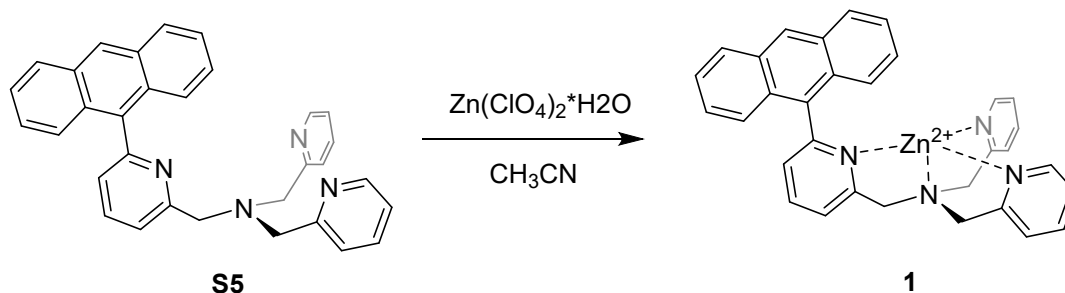
In a Schlenk apparatus, a mixture of (0.276 g, 1.24 mmol), 9-anthraceneboronic acid (0.299 g, 0.81 mmol), Pd(PPh₃)₄ (9.39 mg, 0.82 μmol, 1 mol%) and K₂CO₃ (0.786 g, 5.69 mmol) was dissolved in 15 ml of H₂O/toluene/CH₃OH (1:1:0.5). The mixture was stirred under N₂ for 48 hours at 100°C. The solvent was removed under reduced pressure. The resulting orange oil was dissolved in CHCl₃ and the solution extracted with H₂O (3x20 mL). The organic phases were dried with anhydrous Na₂SO₄, filtered and then the solvent was removed under reduced pressure. The resulting solid was precipitated by crystallization from THF/hexane to yield the product quantitatively as a pale-yellow solid.

¹H-NMR (CDCl₃, 300 MHz); δ(ppm): 8.48 (d, J = 22.7 Hz, 1H), 8.20 – 8.09 (m, 1H), 8.08 – 7.96 (m, 3H), 7.94 – 7.83 (m, 1H), 7.79 – 7.70 (m, 1H), 7.69 – 7.28 (m, 12H), 7.19 – 7.03 (m, 2H), 4.00 (d, J = 19.3 Hz, 6H).

¹³C-NMR (CDCl₃, 75 MHz); δ(ppm): 159.73, 159.17, 157.54, 148.93, 136.81, 136.69, 135.21, 133.84, 131.56, 131.51, 131.25, 130.27, 130.19, 128.82, 128.75, 128.57, 128.29, 127.68, 127.62, 127.32, 127.23, 126.21, 125.85, 125.60, 125.46, 125.30, 125.20, 125.18, 124.91, 123.26, 122.14, 121.69, 77.58, 77.16, 76.74.

ESI-MS (m/z): theoretical mass for [C₃₂H₂₇N₄+H]⁺ = 467.22 m/z; found = 467.41 m/z.

3.3 Synthesis of complex 1



To a suspension of **TPMA** ligand (108.24 mg, 0.23 mmol) in CH₃CN (15 mL) Zn(II) perchlorate hexahydrate was added (98.60 mg, 0.26 mmol). The solution was stirred at room temperature for 1 hour and the reaction was followed by ¹H-NMR and ESI-MS. At the end of the reaction Et₂O (30mL) was added, obtaining the Zn(II) complex quantitatively as a crystalline pale orange solid, then centrifuged and dried.

¹H-NMR (CDCl₃, 300 MHz); δ(ppm): 8.94 (s, 1H), 8.37 (t, J = 7.8 Hz, 1H), 8.28 (d, J = 8.6 Hz, 2H), 8.05 (td, J = 7.8, 1.6 Hz, 2H), 7.83 (d, J = 7.8 Hz, 2H), 7.58 (td, J = 14.9, 6.6 Hz, 6H), 7.36 (dd, J = 7.5, 5.6 Hz, 2H), 7.20 (d, J = 8.8 Hz, 2H), 7.16 – 7.08 (m, 2H), 4.47 – 4.17 (m, 6H).

¹³C-NMR (CDCl₃, 50 MHz); δ(ppm): 158.72, 157.93, 155.39, 148.54, 143.41, 142.68, 132.22, 132.15, 131.39, 131.06, 130.12, 130.10, 129.57, 129.56, 128.09, 127.17, 126.26, 125.85, 125.78, 125.47, 118.31, 118.26, 117.96, 57.90, 57.26.

ESI-MS (m/z): theoretical mass for [C₃₂H₂₆N₄Zn+COOH]⁺ = 575.14 m/z; found = 575.11 m/z; theoretical mass for [C₃₂H₂₆N₄Zn+Cl]⁺ = 565.11 m/z; found = 565.10 m/z.

4. ¹H-NMR and ESI-MS characterization

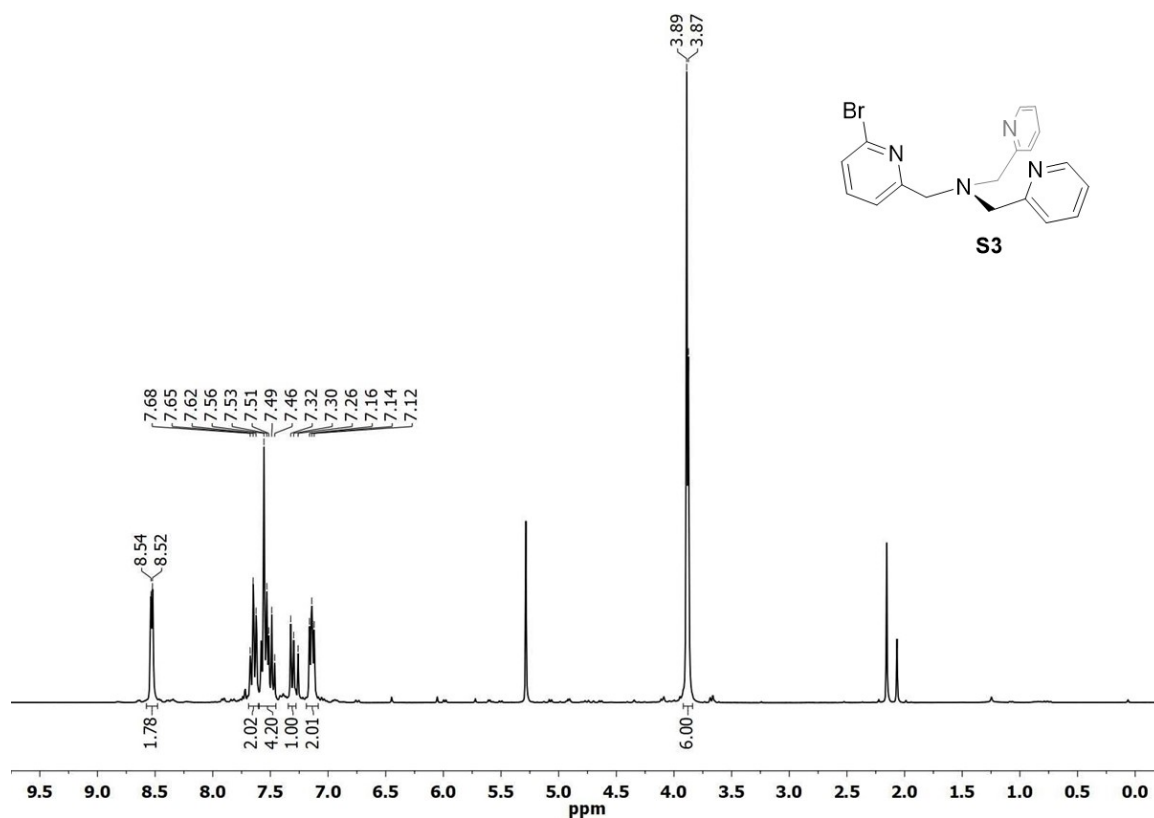


Figure S1. ¹H-NMR spectrum (300 MHz, 301K, CDCl₃) of amine S3.

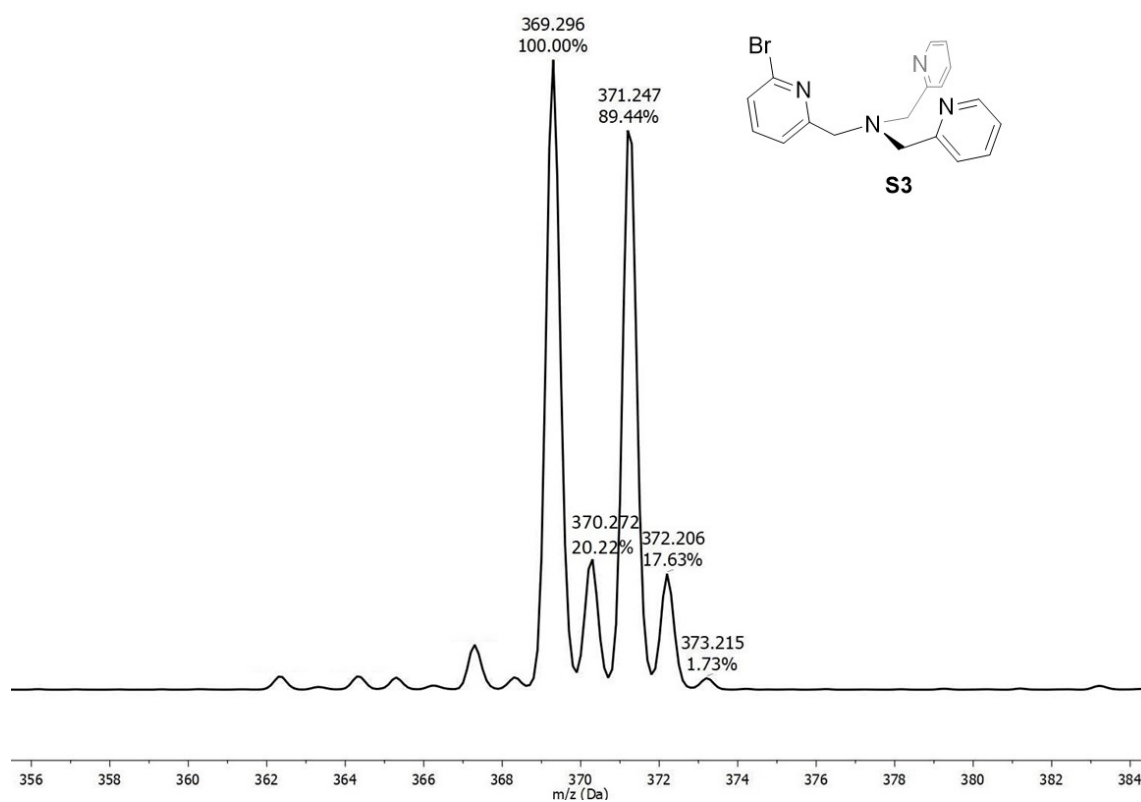


Figure S2. ESI-MS spectrum of amine S3.

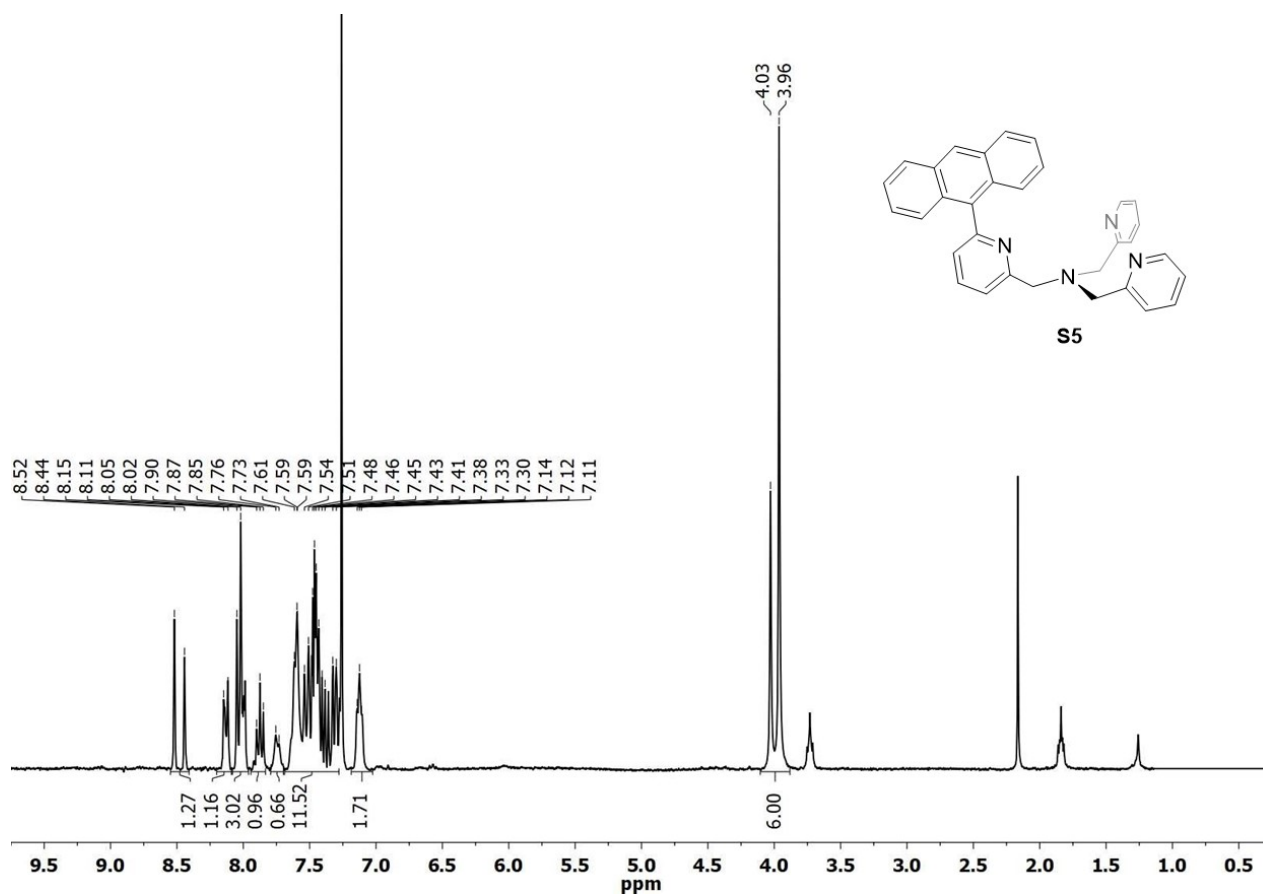


Figure S3. ^1H -NMR spectrum (300 MHz, 301K, CDCl_3) of amine S5.

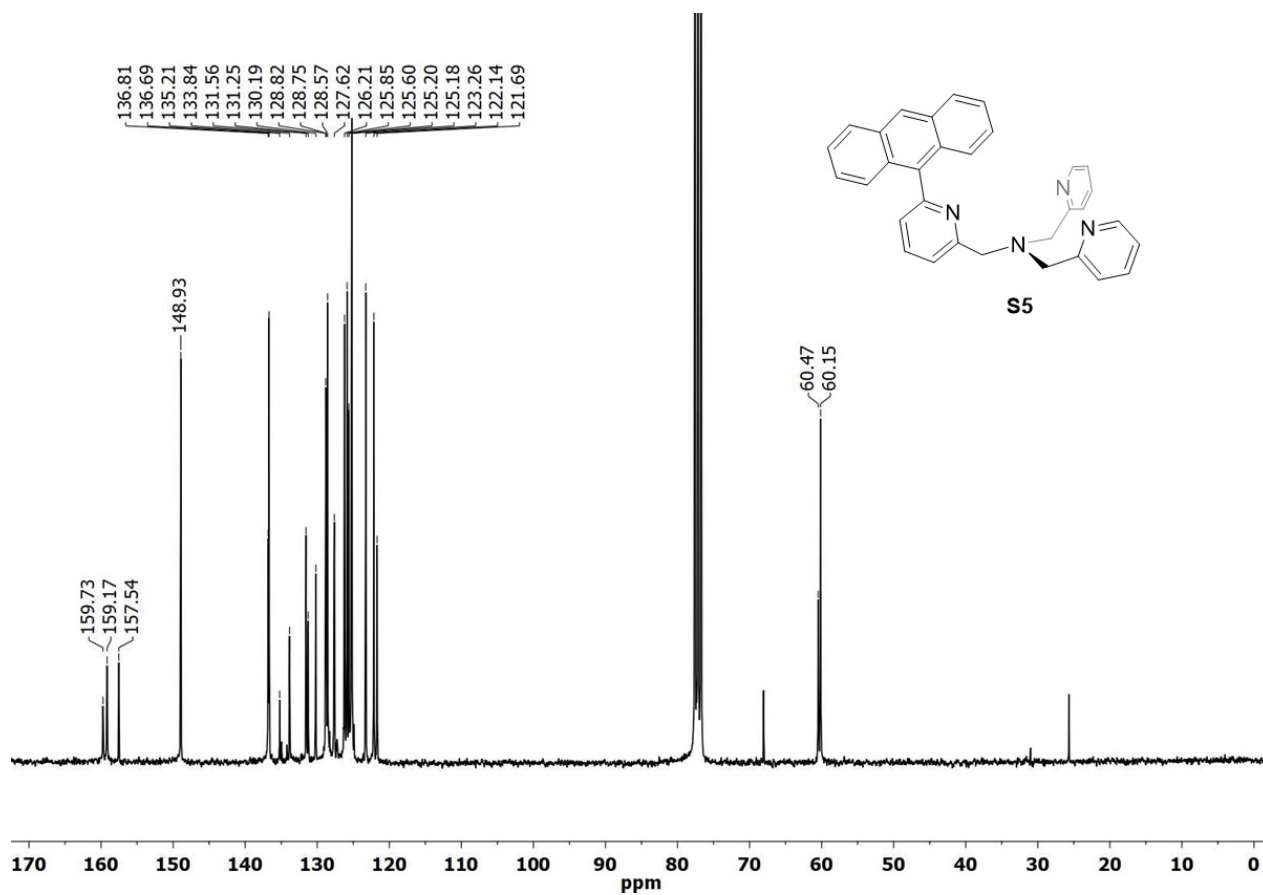


Figure S4. ^{13}C -NMR spectrum (101 MHz, 301K, CDCl_3) of amine S5.

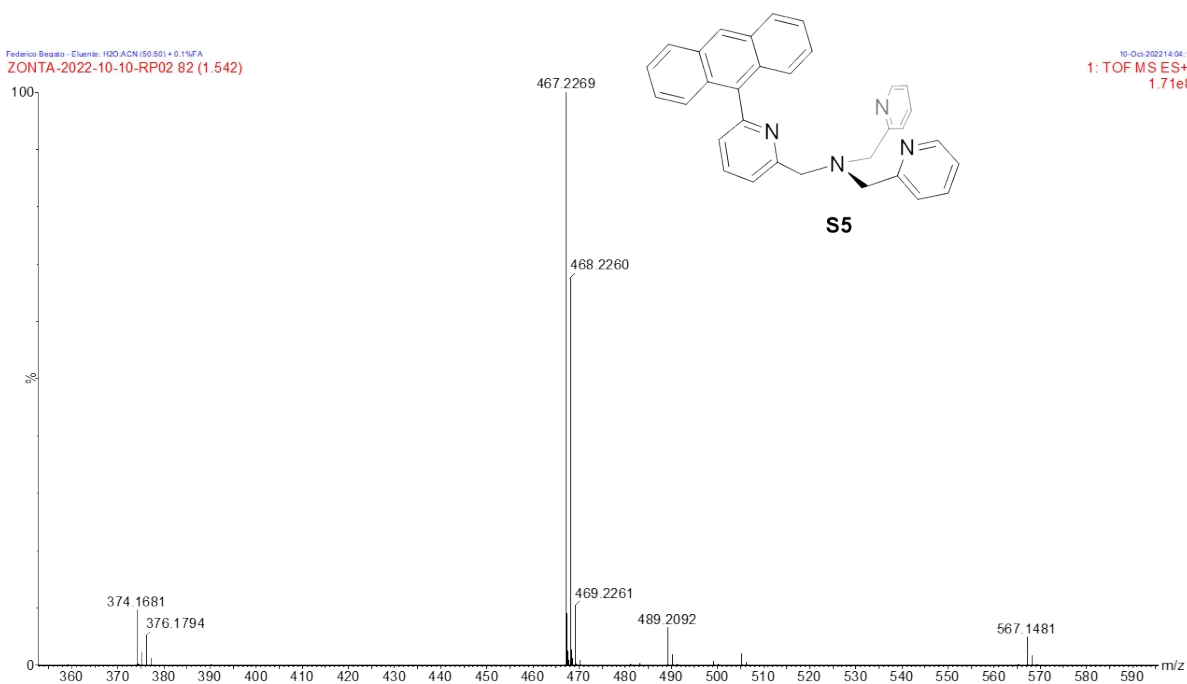


Figure S5. HRMS (ESI-TOF) spectrum of amine S5.

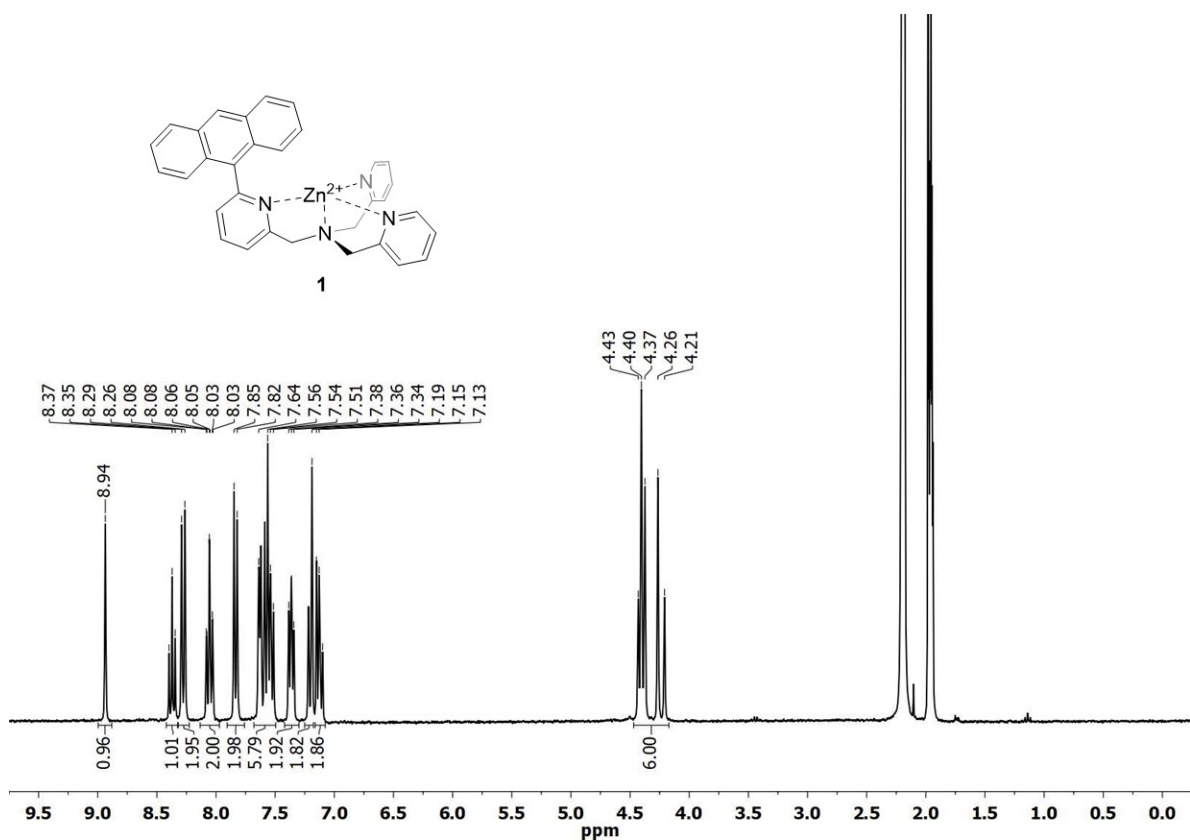


Figure S6. ¹H-NMR spectrum (300 MHz, 301K, CD₃CN) of complex 1.

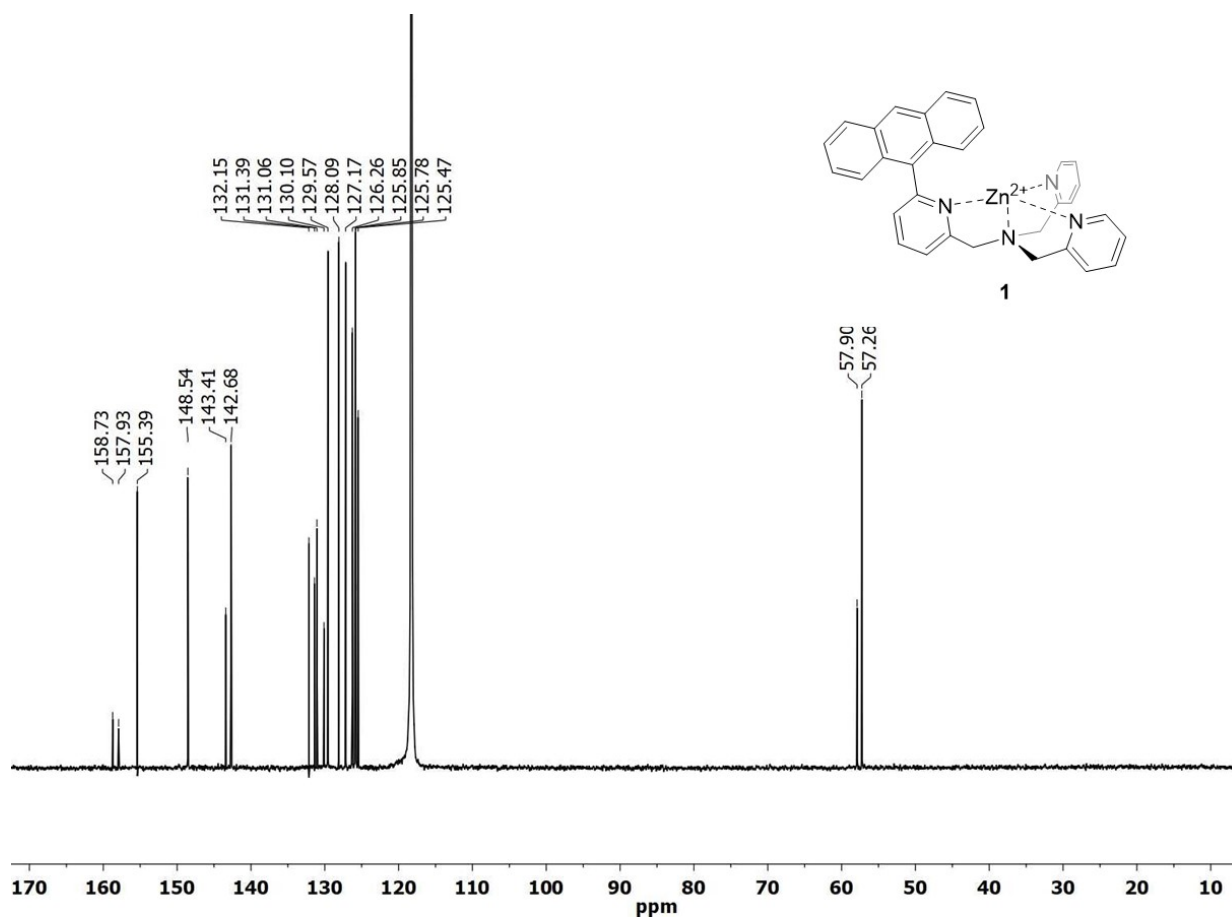


Figure S7. $^{13}\text{C-NMR}$ spectrum (101 MHz, 301K, CD_3CN) of complex 1.

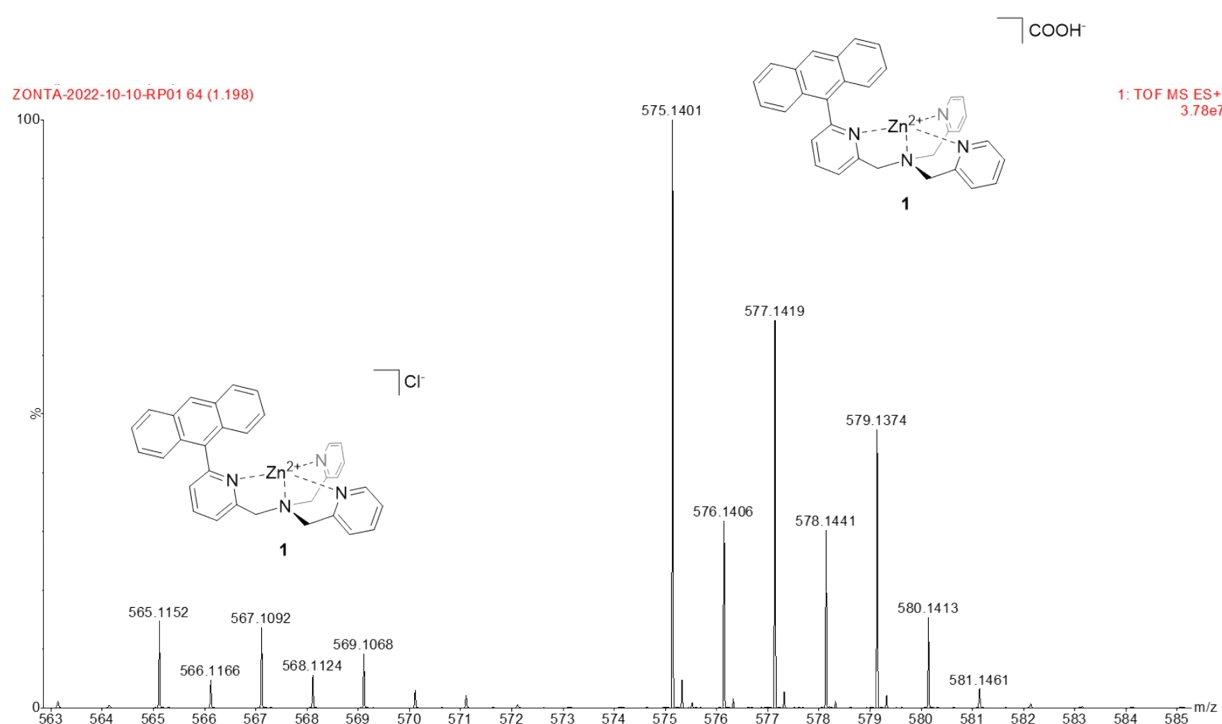


Figure S8. HRMS (ESI-TOF) spectrum of complex 1.

5. UV-Vis Measurements

5.1 Uv-Vis measurements of complex 1

The solution for the UV-Vis measure was prepared from the synthesized complex by dilution in a buffer solution composed by CH₃CN/H₂O 3:1 with HEPES 20 mM to obtain a final concentration equal to 4.0×10^{-5} M (pH=7.4). The spectra were collected with a 1 cm cuvette path length in the range 210 - 400 nm. The UV-Vis spectra is shown in *Figure S9*.

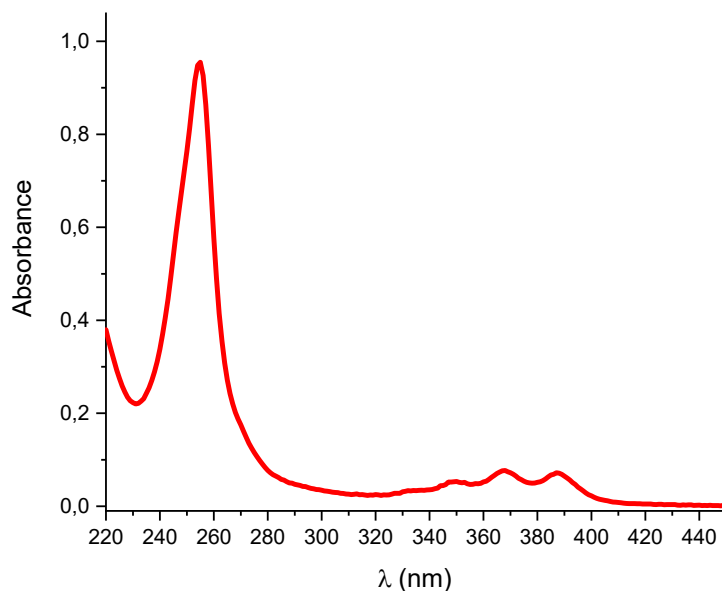
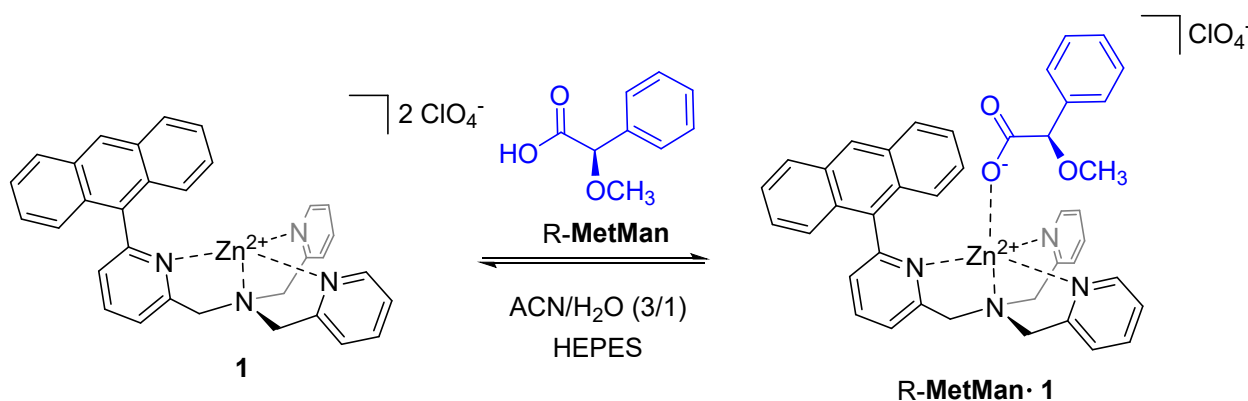


Figure S9. UV-Vis spectrum of complex 1 (4×10^{-5} M) within the range 220 – 440 nm.

5.2 Uv-Vis titration of complex 1 with *R*-methoxyphenylacetic acid *R*-MetMan



The solution for the fluorescent titration was prepared from the synthesized complex by dilution in CH₃CN/H₂O 3:1 with HEPES 20 mM (pH=7.4) to a final concentration of 4×10^{-5} M. The methoxyphenylacetic acid was prepared from the solid by dilution with a solution 4×10^{-5} M of the complex to a concentration in methoxyphenylacetic acid of 10^{-3} M. The complex solution was subsequently titrated with the solution of the acid until a H:G ratio equal to 1:12.8.

The Uv-Vis titration spectra, shown in *Figure S10*, remain approximately constant during the titration, indicating that the complexation of the acid does not have a remarkable impact on the absorbance properties of the complex.

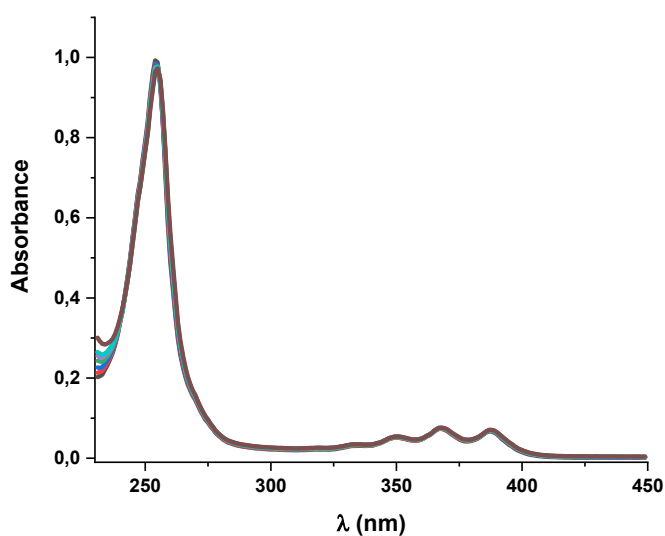


Figure S10. Uv-Vis spectra recorded for the titration of the complex **1** (4.0×10^{-5} M) with *R*-MetMan. The spectra were recorded between 220 and 450 nm for increasing aliquots of the chiral acid ranging from 0 to 12.8 eq. Eight spectra were recorded, respectively with 0.0, 0.2, 0.4, 0.8, 1.6, 3.2, 6.4, 12.8 equivalents of acid added to the complex solution.

5.3 Uv-Vis measurements of a selected series of carboxylic acids

A solution of complex **1** were prepared by dilution in CH₃CN/H₂O 3:1 with HEPES 20 mM (pH=7.4) to a final concentration of 4.0×10^{-5} M. The solution of the acid was prepared by dilution within a solution 4.0×10^{-5} M of complex to a concentration of the chiral acid equal to $2,5 \times 10^{-3}$ M. For the measurements, a defined aliquot of the acid was added to the complex to obtain a concentration of the acid equal to 5×10^{-4} M. The Uv-Vis output were recorded with a 1 cm cuvette path length within the range 250 – 350 nm (*Figure S11*).

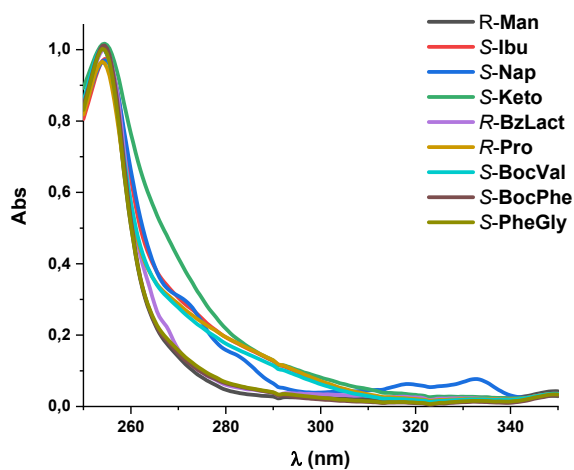


Figure S11. Uv-Vis spectra superposition of the host **1** at concentration of 4.0×10^{-5} M with the nine carboxylate tested at concentration of 5×10^{-4} M.

6. Fluorescence Measurements

The solution for the fluorescent measurements was prepared from the synthesized complex by dilution in CH₃CN/H₂O 3:1 with HEPES 20 mM (pH=7.4) to a final concentration of 5×10^{-6} M. The measure was performed using a 1.0 cm cuvette path length. It was recorded both the excitation fluorescence and the emission fluorescence spectra (*Figure S12* and *Figure S13* respectively). The first were recorded between 220 and 450 nm by setting an emission wavelength equal to 460 nm. Instead, the second were recorded between 260 and 600 nm by setting an excitation wavelength equal to 250 nm.

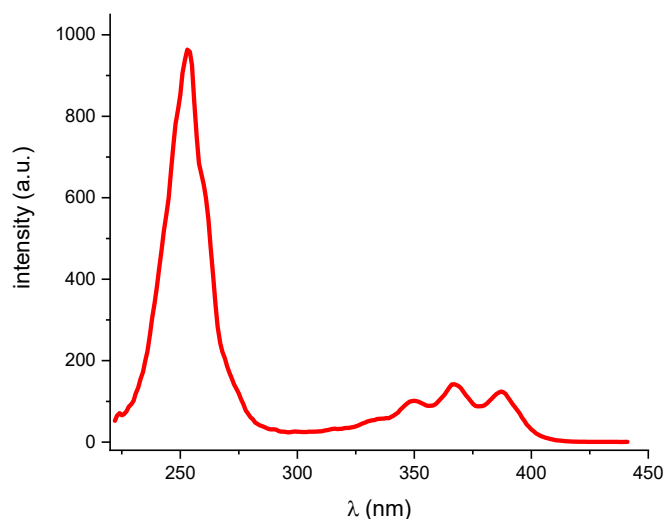


Figure S12. Fluorescence excitation spectrum of complex **1** (5×10^{-6} M) within the range 200-450 nm. Both the excitation and emission slits were fixed at 5 nm.

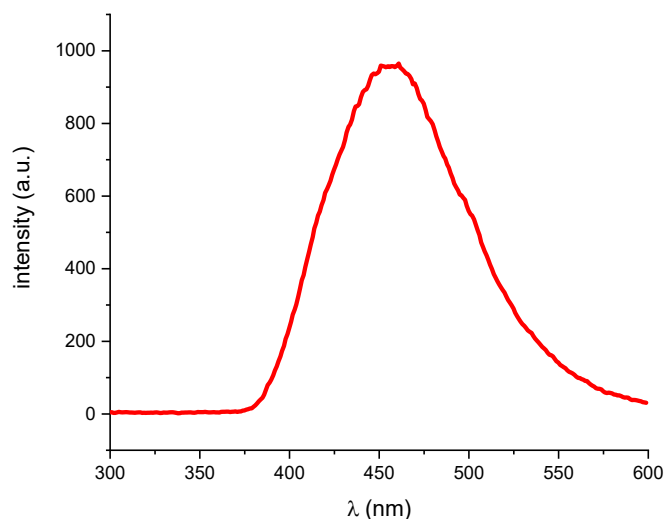
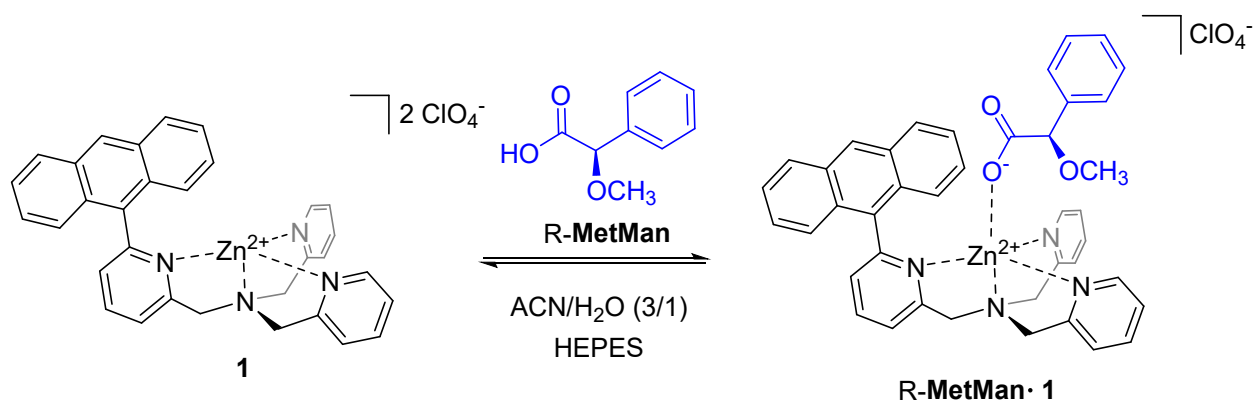


Figure S13. Fluorescence emission spectrum of complex **1** (5×10^{-6} M) within the range 300-600 nm. Both the excitation and emission slits were fixed at 5 nm.

6.1 Fluorescence titration of complex 1 with *R*-methoxyphenylacetic acid *R*-MetMan



The solution for the fluorescent titration was prepared from the synthesized complex by dilution in $\text{CH}_3\text{CN}/\text{H}_2\text{O}$ 3:1 with HEPES 20 mM (pH=7.4) to a final concentration of 5×10^{-6} M. The methoxyphenylacetic acid was prepared from the solid by dilution with a solution 5×10^{-6} M of the complex to a concentration in methoxyphenylacetic acid of 5×10^{-4} M. The complex solution was subsequently titrated with the solution of the acid until a H:G ratio equal to 1:12.8.

The fluorescence titration spectra are shown in *Figure S14*. Both the excitation and the emission of fluorescence spectra remain approximately constant during the titration, indicating that the complexation of the acid does not have a remarkable impact on the fluorescent properties of the complex. Moreover, the excitation fluorescence spectra show the same bands with the same relative intensities of the absorbance spectra of the complex (*Figure S9*). This is expected since the zinc complex is the only species that absorbs and emits in solution.

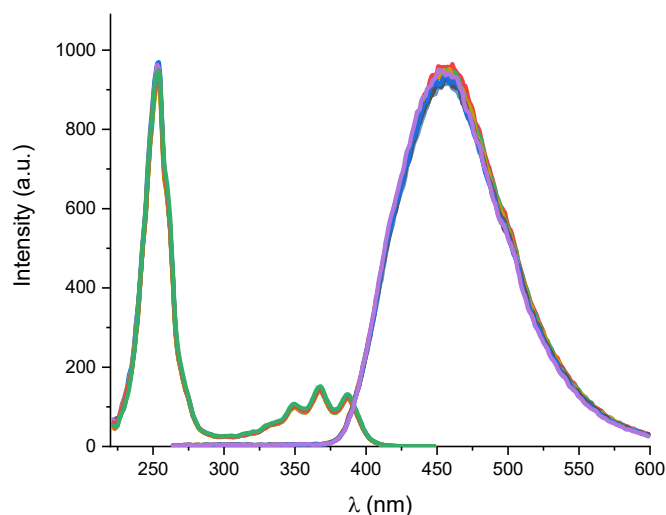


Figure S14. Fluorescent excitation (*left*) and emission (*right*) spectra recorded for the titration of the complex **1** (5.0×10^{-6} M) with *R*-MetMan. The spectra were recorded between 220 and 600 nm for increasing aliquots of the chiral acid ranging from 0 to 12.8 eq. Eight excitation and emission spectra were recorded, respectively with 0.0, 0.2, 0.4, 0.8, 1.6, 3.2, 6.4, 12.8 equivalents of acid added to the complex solution. Both the excitation and emission slits were fixed at 5 nm.

6.2 Fluorescence measurements in the presence of the “chiroptical contaminant” *R*-BINAPO and complex **1**

The fluorescence measurements of the chiroptical contaminant chosen for the CD and FDCD experiment was performed to check if the complex **1** is the only emitting species above 420 nm (filter used for FDCD measurements).

A solution containing complex **1** (10^{-5} M) and *R*-BINAPO (5×10^{-4} M) was prepared and analysed. The *R*-BINAPO species has an excitation band with a maximum at 252 nm while an emission band centred at around 350 nm (Figure S15).

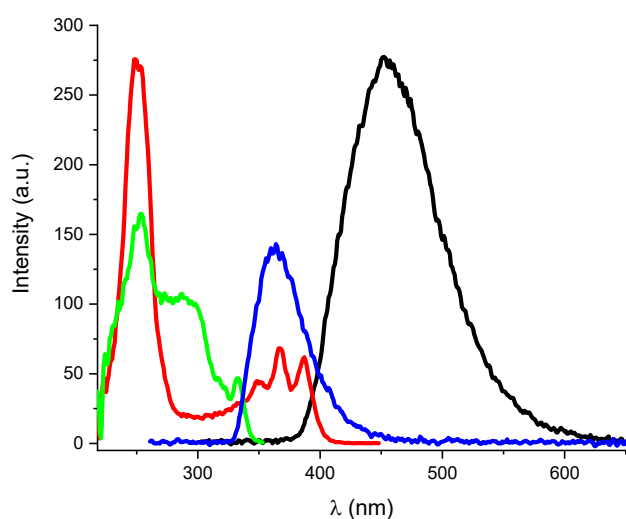


Figure S15. Fluorescence excitation spectra of complex **1** (red, 10^{-5} M) and *R*-BINAPO (green, 5×10^{-4} M) and fluorescence emission spectra of complex **1** (black, 10^{-5} M) and *R*-BINAPO (blue, 5×10^{-4} M). The excitation slit was fixed at 2,5 nm while the emission slit at 5,0 nm. (5×10^{-6} M)

6.3 Fluorescence measurements in the presence of the “chiroptical contaminant” (-)-Riboflavin and complex 1

A second chiroptical contaminant was tested. This one is emitting within the range of the probe (400-550 nm). The fluorescence properties of the (-)-Riboflavin was tested preparing a solution by dilution in CH₃CN/H₂O 3:1 with HEPES 20 mM (pH=7.4) to a final concentration of 10⁻⁵ M (Figure S16).

The interference the Riboflavin to the fluorescence of the complex 1 was tested through a titration experiment. The solution for the fluorescent titration was prepared from the synthesized complex by dilution in CH₃CN/H₂O 3:1 with HEPES 20 mM (pH=7.4) to a final concentration of 10⁻⁵ M. The (-)-Riboflavin solution was prepared from the solid by dilution with a solution 10⁻⁵ M of the complex to a concentration in (-)-Riboflavin of 5×10⁻³ M. The complex solution was subsequently titrated until a final concentration of the contaminant equal to 5×10⁻³ M. At each step of the titration was recorded the excitation an emission spectra of both the complex 1 and the (-)-Riboflavin contaminant. This was done by setting different emission (455 and 520 nm for the complex 1 and the (-)-Riboflavin respectively) and excitation (250 and 460 nm for the complex 1 and the (-)-Riboflavin respectively) wavelength (Figure S17).

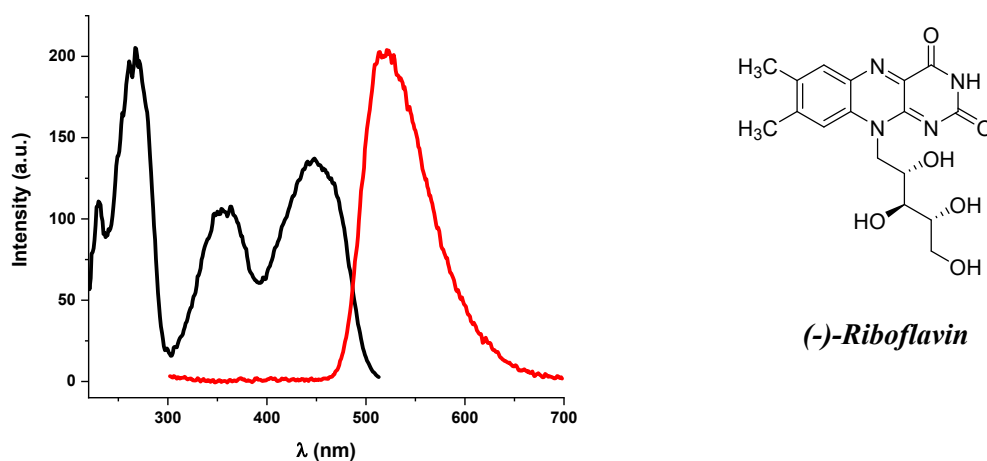


Figure S16. Fluorescence excitation (black) and emission (red) spectra of (-)-Riboflavin (5×10⁻⁵ M). Both the excitation and emission slits were fixed at 2,5 nm.

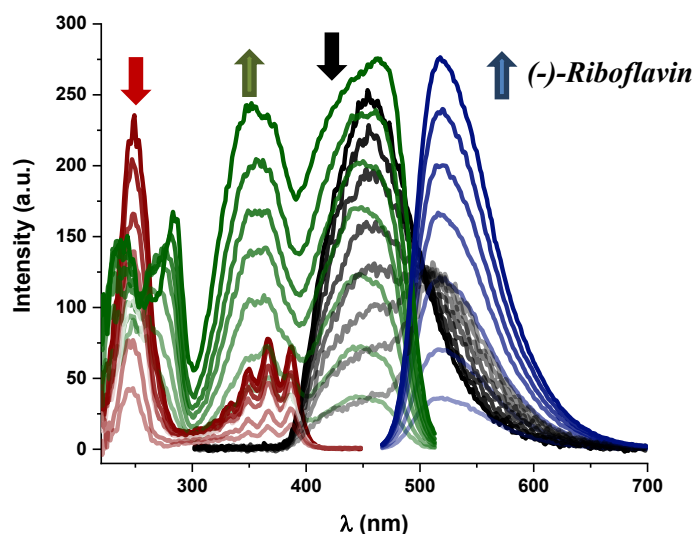


Figure S17. Fluorescent excitation (left, red and green for the complex 1 and (-)-Riboflavin respectively) and emission (right, black and blue for the complex 1 and (-)-Riboflavin respectively) spectra recorded for the titration of the complex 1 (10⁻⁵ M) with (-)-Riboflavin. The spectra were recorded between 220 and 700 nm for increasing aliquots of the chiral chiroptical contaminant ranging from 0 M to 5×10⁻⁴ M.

7. ECD measurements

7.1 ECD titration complex **1** (10^{-5} M) with *R*-methoxyphenylacetic acid *R*-MetMan

The solution for the circular dichroism measurements was prepared from the synthesized complex by dilution in $\text{CH}_3\text{CN}/\text{H}_2\text{O}$ 3:1 with HEPES 20 mM (pH=7.4) to a final concentration of 10^{-5} M. The solution of the acid was prepared by dilution within a solution 10^{-5} M of complex to a concentration of the chiral acid equal to 2×10^{-4} M. A defined aliquot of the acid solution was then added to the complex in the range H:G ratio equal to 1:10. CD data were recorded with a 1.0 cm cuvette path length within the range 250 – 320 nm. CD spectra and fitting are reported in *Figure S18* while the binding constant value was found to be $3000 \text{ M}^{-1} \pm 300 \text{ M}^{-1}$.

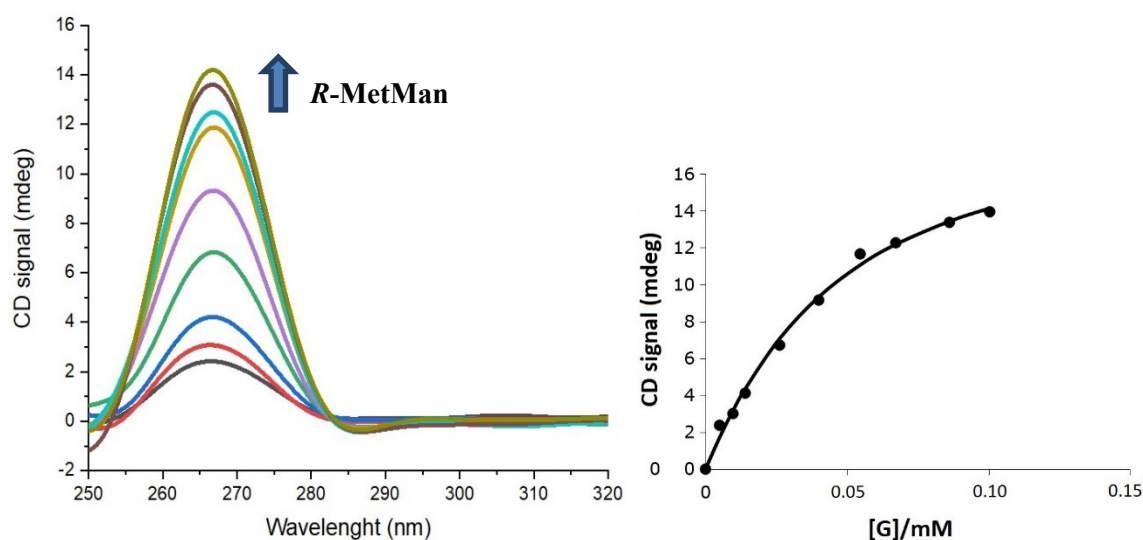


Figure S18. ECD spectra (left) and fitting (right) for the *R*-MetMan·**1** host-guest titration. The analyzed solution of **1** was 10^{-5} M with increasing concentration of *R*-MetMan as reported in the plot; the cuvette used for the measurements was 1 cm. The solutions were prepared in buffer 3:1 $\text{H}_2\text{O}/\text{CH}_3\text{CN}$ with HEPES 20 mmol. The sample compartment was thermostated at 298 K. The fitting was performed considering a 1:1 binding model.

7.2 ECD titration of complex **1** (2×10^{-4} M) with *S*-methoxyphenylacetic acid *S*-MetMan

The experiment showed in the previous section was repeated with a higher host concentration, this time to verify the presence of the signal at 300 nm observed in the FDCD titration measurement (see section 7.1). The solution was prepared from the synthesized complex by dilution in $\text{CH}_3\text{CN}/\text{H}_2\text{O}$ 3:1 with HEPES 20 mM (pH=7.4) to a final concentration of 2×10^{-4} M. The solution of the acid was prepared by dilution within a solution 2×10^{-4} M of complex to a concentration of the chiral acid equal to 2×10^{-3} M. A defined aliquot of the acid solution was then added to the complex to obtain a H:G ratio equal to 1:10. The CD data were recorded with a 1.0 cm cuvette path length within the range 275 – 420 nm. CD spectra and fitting are reported in *Figure S19*. The broad signal between 290 – 410 nm is clearly visible upon the addition of the chiral *S*-MetMan acid. This is also in good accordance with the theoretical spectra prediction showed in section 10.

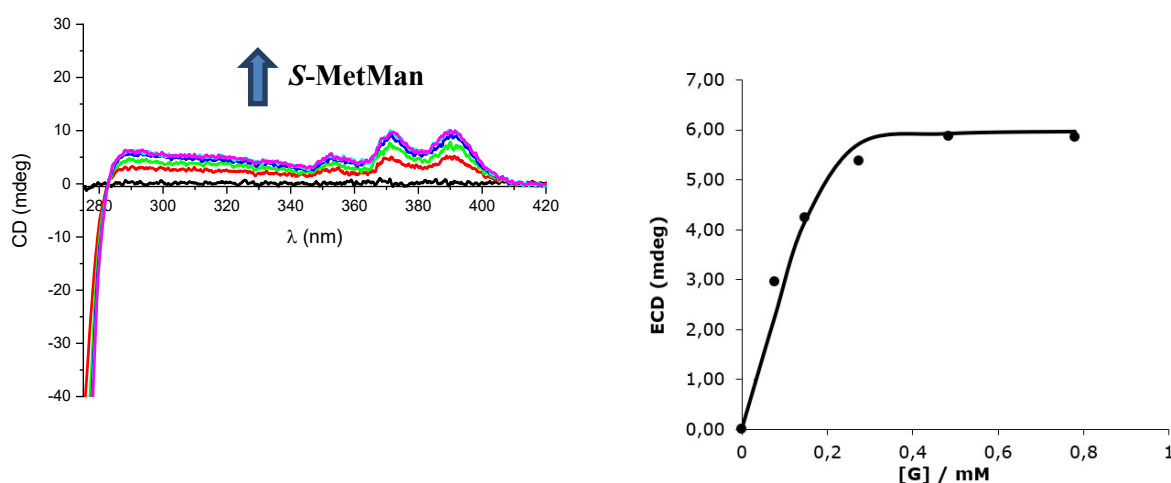


Figure S19. ECD spectra (left) and fitting (right) for the *S*-MetMan·**1** host-guest titration. The analyzed solution of **1** was 2×10^{-4} M (2 mL) while the H:G ratio was 1:10 and the cuvette used for the measurements was 1 cm. The solutions were prepared in buffer 3:1 $\text{H}_2\text{O}/\text{CH}_3\text{CN}$ with HEPES 20 mmol. The sample compartment was thermostated at 298 K.

7.3 ECD sensing capability

Three solutions at different concentration of the complex **1** were prepared by dilution in CH₃CN/H₂O 3:1 with HEPES 20 mM (pH=7.4) to a final concentration equal to 10⁻⁵ M, 10⁻⁶ M, and 10⁻⁷ M. The solution of the acid was prepared by dilution to a concentration of the chiral acid equal to 2,5×10⁻³ M. For the measurements, a defined aliquot of the acid was added to the complex to obtain a concentration of the acid equal to 5×10⁻⁴ M. The CD output were recorded with a 1 cm cuvette path length within the range 250 – 320 nm (*Figure 1b*).

7.4 ECD measurements of a selected series of carboxylic acids

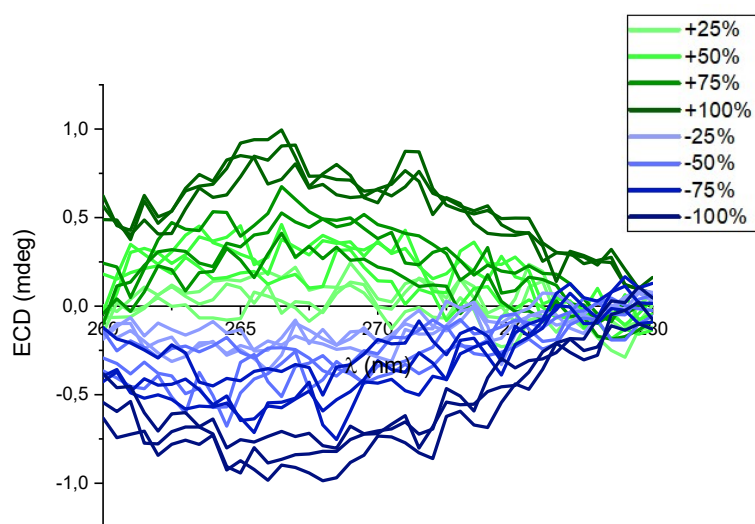
A solution of complex **1** were prepared by dilution in CH₃CN/H₂O 3:1 with HEPES 20 mM (pH=7.4) to a final concentration of 10⁻⁵ M. The solution of the acid was prepared by dilution within a solution 10⁻⁵ M of complex to a concentration of the chiral acid equal to 2,5×10⁻³ M. For the measurements, a defined aliquot of the acid was added to the complex to obtain a concentration of the acid equal to 5×10⁻⁴ M. The HT(V) value of the phototube was fixed to 570 for all the measurements. The CD output were recorded with a 1 cm cuvette path length within the range 250 – 320 nm (*Figure 1c*)

7.5 Enantiomeric excess calibration curve of MetMan acid versus CD amplitude

The limit of complex **1** to act as stereodynamic probe was tested preparing a calibration curve with a concentration of **1** equal to 10^{-6} M. Six solutions were prepared using complex **1** at 10^{-6} M and the acid **MetMan** 5×10^{-4} M at six different *e.e.* (+100%, +75%, +25%, -25%, -75%, -100%).

Eight curves were recorded and a linear relationship was obtained between the ellipticity value recorded by the ECD spectrometer (mean value between 265 and 275 nm) and the *e.e.*(%) of the chiral acid **MetMan** (Figure S20). The measurements were repeated three times. From these, the calibration line and the confidence band were obtained from the least squares regression analysis.

a)



b)

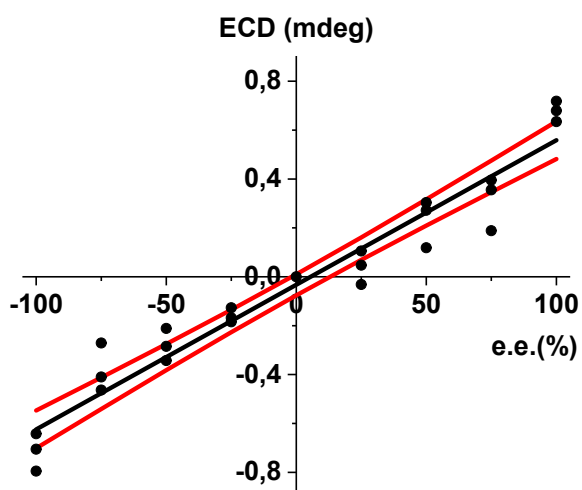


Figure S20. a) ECD spectra between 260 and 280 nm of complex **1** (10^{-6} M) in the presence of **MetMan** acid (5×10^{-4} M) at different enantiopurities. b) Calibration curve (black line) and confidence bands (red lines) of **MetMan** acid *ee*(%) with respect to the ellipticity mean value recorded between 265-275 nm. The fitting equation curve is $y=0.0059x+0.033$, $R^2=0.94$.

7.6 ECD titration of complex **1** (10^{-5} M) and *R*-MetMan (5×10^{-4} M) acid with *R*-BINAPO

ECD titration of complex **1** and *R*(or *S*)-MetMan acid with additional aliquots of *R*-BINAPO was performed to test the influence of this interfering species on the CD output of the adduct *R*-MetMan•**1**. A solution containing complex **1** (10^{-5}) and *R*(or *S*)-MetMan (5×10^{-4} M) acid was prepared by dilution from the pure compounds in CH₃CN/H₂O 3:1 with HEPES 20 mM (pH=7.4) as previously described. The solution of *R*-BINAPO was prepared by dilution within a solution 10^{-5} M of complex to a concentration of *R*-BINAPO equal to 2×10^{-3} M. A defined aliquot *R*-BINAPO solution was then added to the solution containing complex **1** and *R*(or *S*)-MetMan to obtain a final concentration of *R*-BINAPO equal to 5×10^{-4} M. The CD output were recorded with a 1.0 cm cuvette path length within the range 250 – 350 nm. G-value, CD spectra (mdeg), and Abs response are reported in Figure S21.

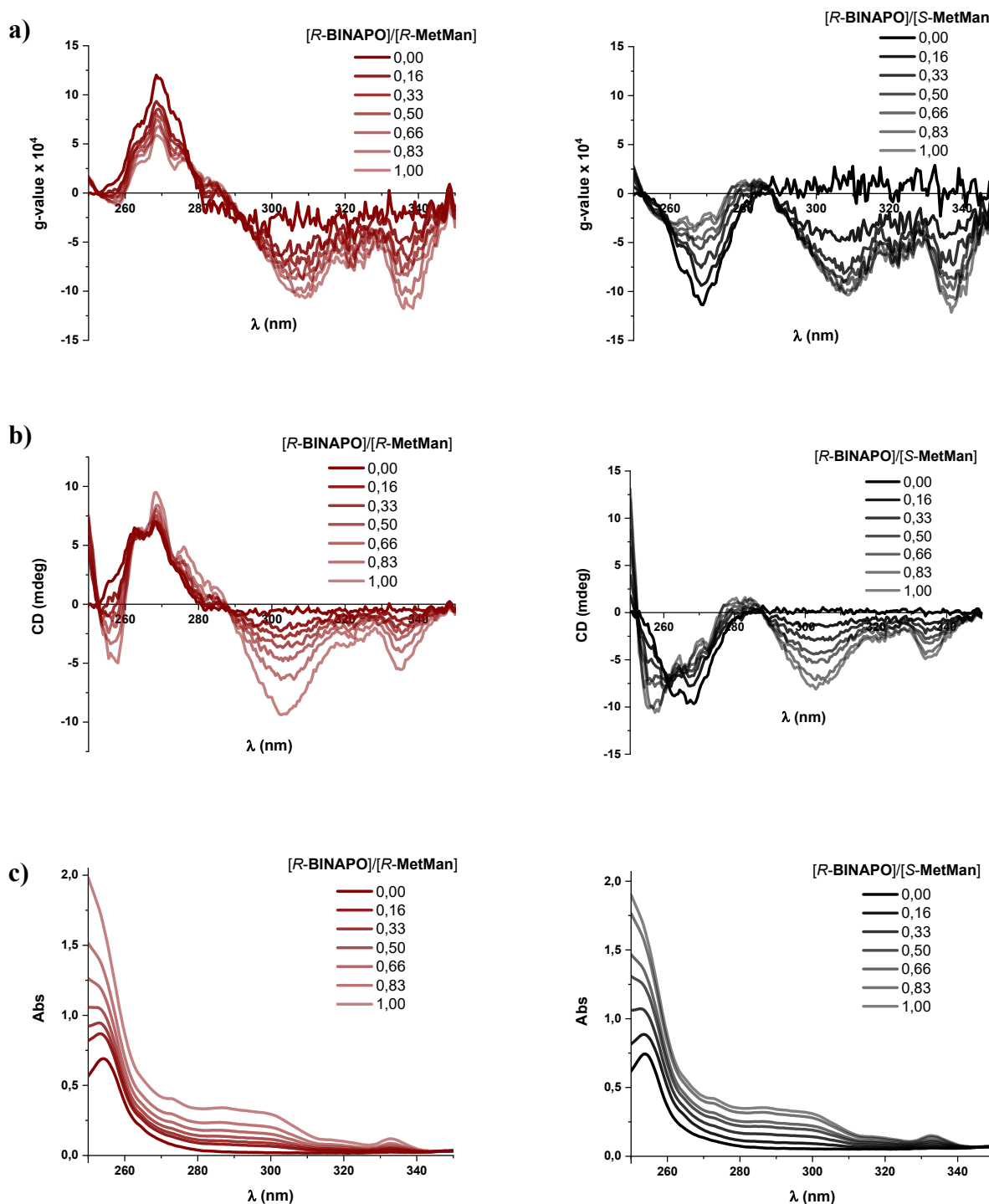


Figure S21. a) g-value, b) CD (mdeg), and c) Abs spectra for the titration of the host **1** (10^{-5} M) and *R*(left) or *S*(right)-MetMan acid (5×10^{-4} M) with additional aliquots of *R*-BINAPO (from 0 M (solid line) to 5×10^{-4} M (faded line)).

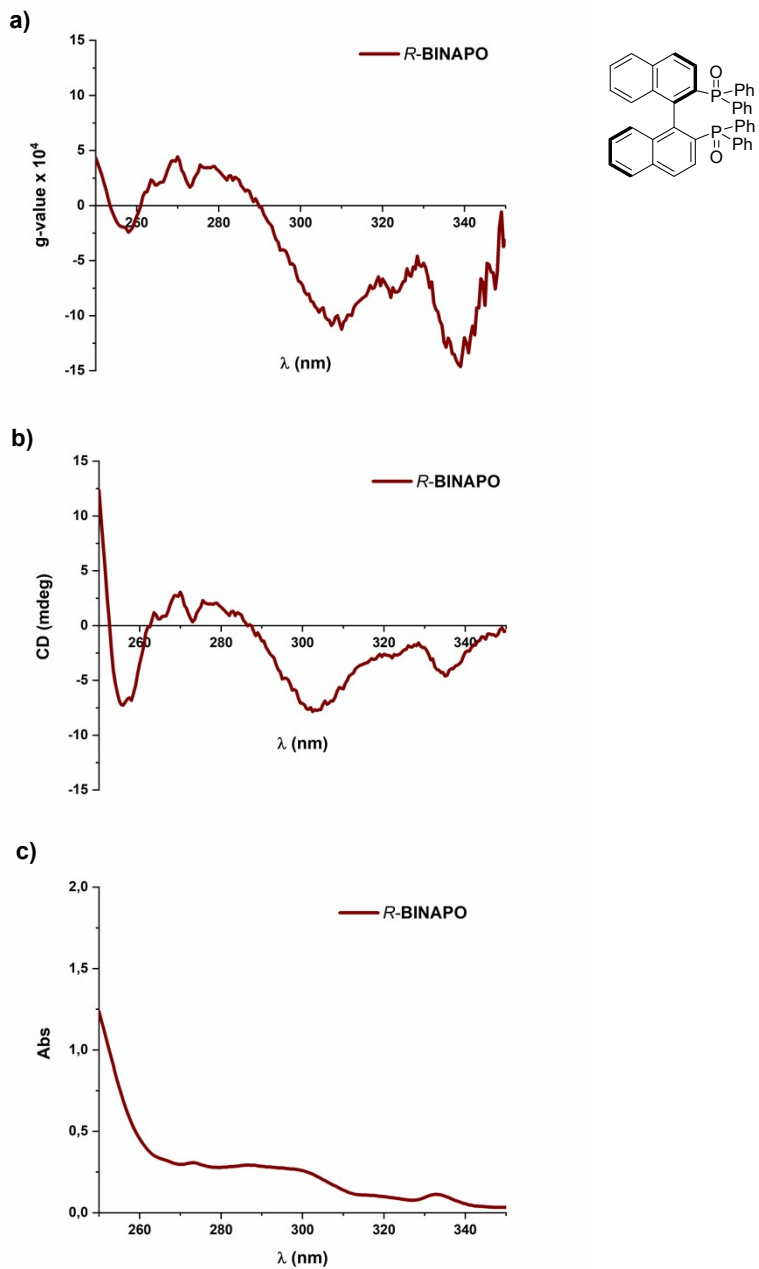


Figure S22 a) g-value, b) CD (mdeg), and c) Abs spectra of the “chiroptical contaminant” *R*-BINAPO at a concentration equal to 5×10^{-4} M.

8. FDCD measurements

All the solutions for the FDCD measurements were prepared using as solvent a buffer solution made by dissolving 4-(2-hydroxyethyl)-1-piperazineethanesulfonic acid HEPES to a final concentration equal to 20 mM in CH₃CN/H₂O 3:1 and adjusting the pH to 7.4 with NaOH 1 M. The FDCD measurements were performed with a CD spectrometer Jasco J-1500 changing the position of the photomultiplier (PM) detector to a 90° geometry in respect to the direction of the excitation light source. Instead, a photodiode (PD) detector was placed at 180° geometry. The high tension (HT) voltage of the detector was adjusted for each measurements to optimize the direct current (DC) output of the instrument, corresponding to the total fluorescence of the system. To register the FDCD spectra, the following parameters were set: D.I.T. 2 sec, bandwidth 10 nm, scanning speed 50 nm/min, acquisition range 250 – 320 nm, cuvette path length 1 cm. A 420 nm high-pass filter were inserted between the sample and the PM detector to avoid the collection of scattered light from the sample.

8.1 FDCD titration complex 1 with *R*-methoxyphenylacetic acid *R*-MetMan

The solution for the FDCD measurements was prepared from the synthesized complex by dilution in CH₃CN/H₂O 3:1 with HEPES 20 mM (pH=7.4) to a final concentration of 10⁻⁴ M. The solution of the acid was prepared by dilution within a solution 10⁻⁴ M of complex to a concentration of the chiral acid equal to 10⁻² M. A defined aliquot of the acid solution was then added to the complex to obtain a H:G ratio equal to 1:24.

The binding constant ($K=4100 \text{ M}^{-1} \pm 200 \text{ M}^{-1}$) was obtained from the fitting of the FDCD value (mdeg) registered between 300-310 nm versus the equivalent of acids added assuming a 1:1 adduct between the complex **1** and the *R*-MetMan acid (*Figure S23*). The *K* determination within this region of the spectra is not influenced by the self-absorption of the tripyridyl system that occurs at 275 nm.

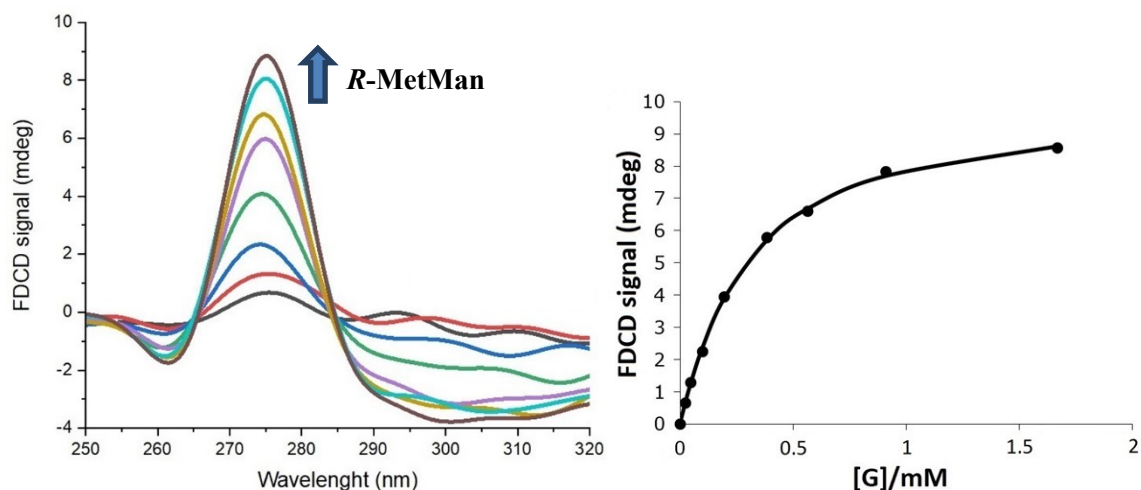


Figure S23. FDCD spectra (left) and fitting (right) for the *R*-MetMan·**1** host-guest titration. The analyzed solution of **1** was 10⁻⁴ M with increasing concentration of *R*-MetMan as reported in the plot; the cuvette used for the measurements was 1 cm. The buffer was a 3:1 H₂O/CH₃CN solution in which HEPES was dissolved at a concentration of 20 mmol. The sample compartment was thermostated at 298 K. The phototube working voltage was set at 550 V. The fitting was performed considering a 1:1 binding model.

8.2 FDCD sensing capability

Four solutions at different concentration of the complex **1** were prepared by dilution in CH₃CN/H₂O 3:1 with HEPES 20 mM (pH=7.4) to a final concentration equal to 10⁻⁵ M, 10⁻⁶ M, and 10⁻⁷ M. The solution of the acid was prepared by dilution to the desired final concentration of a chiral acid solution initially at 2,5×10⁻³ M. For the measurements, a defined aliquot of the acid was added to the complex to obtain a concentration of the acid equal to 5×10⁻⁴ M. The HT(V) of the PM detector was adjust to 550 V and 690 V and 790 V values respectively for the 10⁻⁵ M, 10⁻⁶ M, and 10⁻⁷ M measurements. The FDCD output were recorded with a 1 cm cuvette path length within the range 250 – 320 nm (*Figure 2a*).

8.3 FDCD measurements of a selected series of carboxylic acids

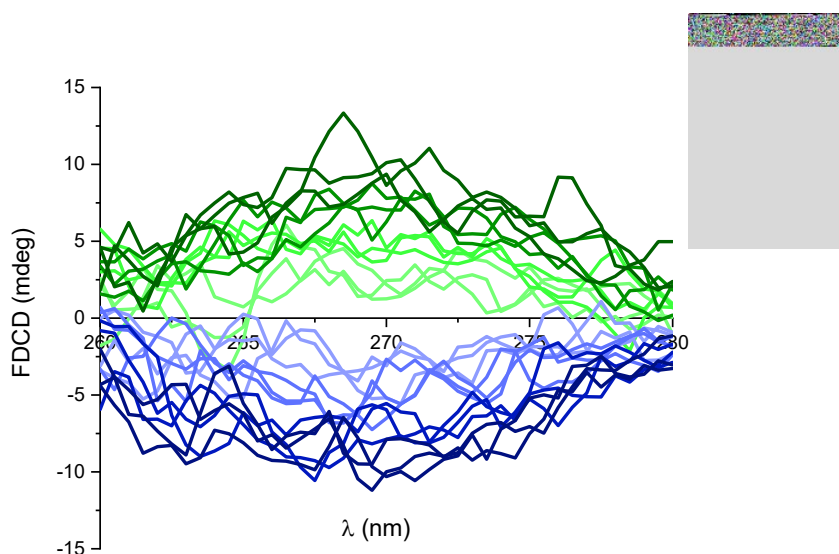
A solution of complex **1** were prepared by dilution in CH₃CN/H₂O 3:1 with HEPES 20 mM (pH=7.4) to a final concentration of 10⁻⁵ M. The solution of the acid was prepared by dilution within a solution 10⁻⁵ M of complex to a concentration of the chiral acid equal to 2,5×10⁻³ M. For the measurements, a defined aliquot of the acid was added to the complex to obtain a concentration of the acid equal to 5×10⁻⁴ M. The FDCD output were recorded with a 1 cm cuvette path length within the range 250 – 320 nm (*Figure 2b*).

8.4 Enantiomeric excess calibration curve of MetMan acid versus FDCD amplitude

To test the limit of complex **1** to act as stereodynamic probe was tested preparing a calibration curve via FDCD with a concentration of **1** equal to 10^{-7} M. Six solutions were prepared using complex **1** at 10^{-7} M and the acid **MetMan** 5×10^{-4} M at eight different *e.e.* (+100%, +75%, +25%, -25%, -75%, -100%).

Eight curves were recorded between 260 and 280 nm and a linear relationship was obtained between the ellipticity value recorded by the FDCD spectrometer (mean value between 265 and 275 nm) and the *e.e.*(%) of the chiral acid **MetMan** (Figure S24). The measurements were repeated three times. From these, the calibration line and the confidence band were obtained from the least squares regression analysis.

a)



b)

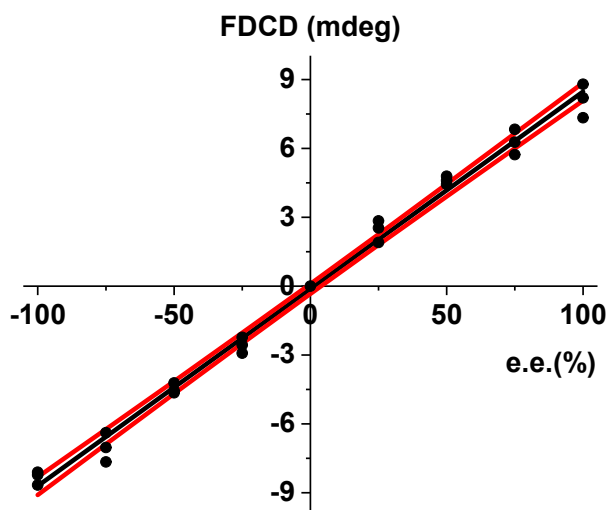


Figure S24. a) FDCD spectra between 260 and 280 nm of complex **1** (10^{-7} M) in the presence of **MetMan** acid (5×10^{-4} M) at different enantiopurities. The HT(V) value was fixed to 750 for all the measurements. b) Calibration curves (black line) and confidence bands (red lines) of **MetMan** acid *ee*(%) with respect to the ellipticity mean value recorded between 265-275 nm. The fitting equation curve is $y=0.086x+0.12$, $R^2=0.99$.

8.5 FDCD titration of complex **1** (10^{-5} M) and *R*-MetMan (5×10^{-4} M) acid with *R*-BINAPO

FDCD titration of complex **1** and *R*(or *S*)-MetMan with additional aliquots of *R*-BINAPO was performed to test the influence of this interfering species on the FDCD output of the adduct *R*(or *S*)-MetMan•**1**. The same procedure adopted in section 6.5 for ECD measurement was adopted. A solution containing complex **1** (10^{-5}) and *R*(or *S*)-MetMan (5×10^{-4} M) acid was prepared by dilution from the pure compounds in CH₃CN/H₂O 3:1 with HEPES 20 mM (pH=7.4). The solution of *R*-BINAPO was prepared by dilution within a solution 10^{-5} M of complex to a concentration of *R*-BINAPO equal to 2×10^{-3} M. A defined aliquot *R*-BINAPO solution was then added to the solution containing complex **1** and *R*(or *S*)-MetMan to obtain a final concentration of *R*-BINAPO equal to 5×10^{-4} M. The FDCD output were recorded with a 1.0 cm cuvette path length within the range 250 – 350 nm. The HT(V) of the phototube detector was fixed to 550 for all the measurements. FDCD/DC, FDCD spectra (mdeg), and DC(V) response are reported in Figure S25.

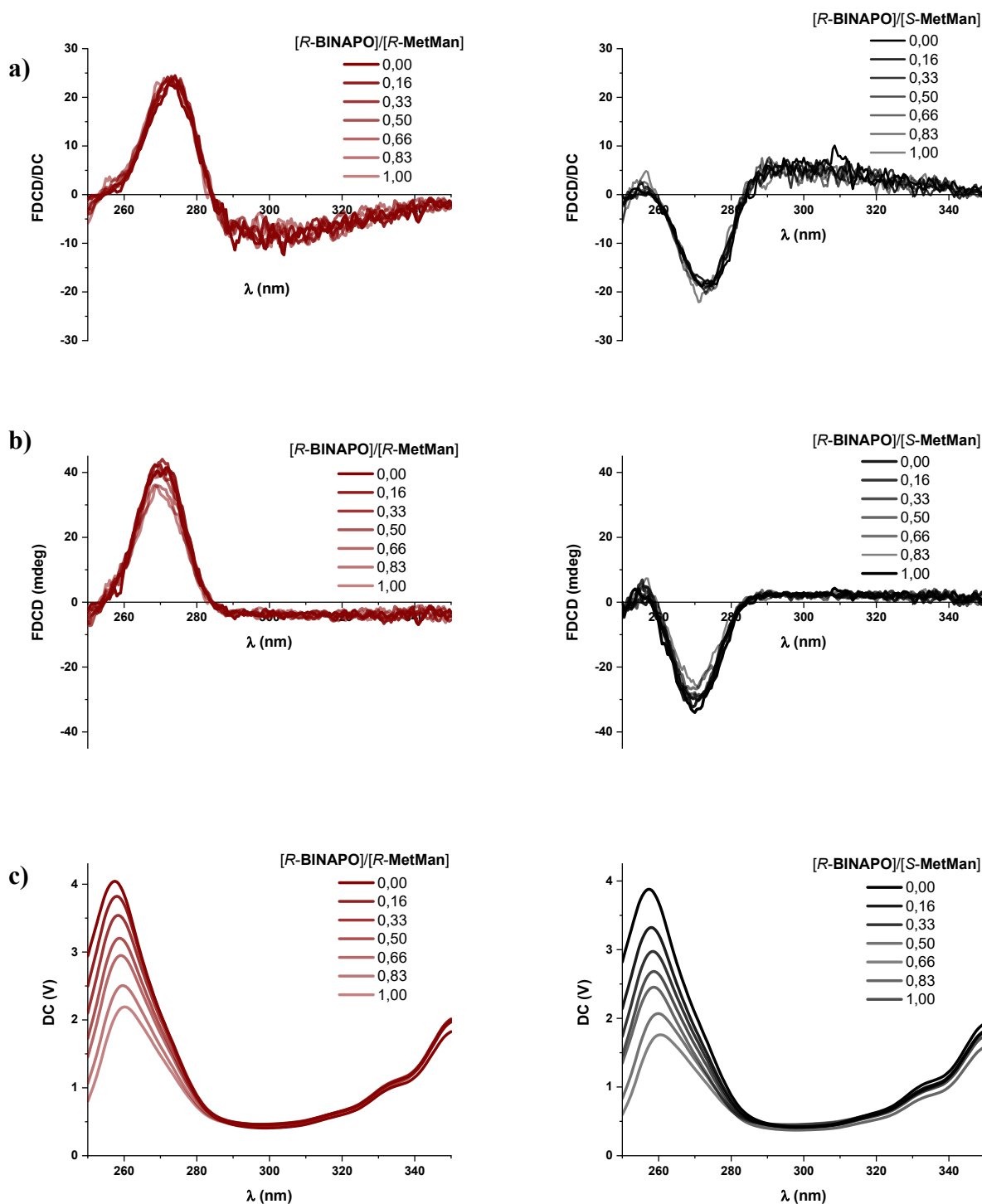


Figure S25. a) FDCD/DC, b) FDCD (mdeg), and c) DC (V) spectra for the titration of the host **1** (10^{-5} M) and *R*(left) or *S*(right)-MetMan acid (5×10^{-4} M) with additional aliquots of *R*-BINAPO (from 0 M (solid line) to 5×10^{-4} M (faded line)).

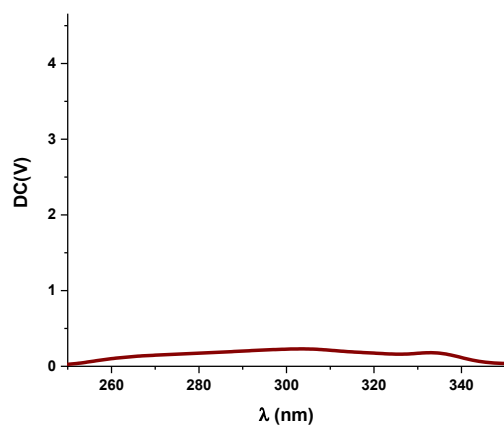
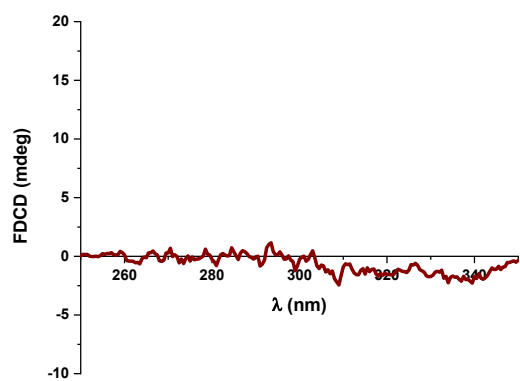


Figure S26. a) FDCD/DC and b) FDCD (mdeg) spectra of the “chiroptical contaminant” *R*-**BINAPO** at a concentration equal to 5×10^{-4} M. FDCD/DC ratio was not reported since the low value of the DC(V) makes it not reliable.

8.6 FDCD titration of complex **1** (10^{-5} M) and *R*-MetMan (5×10^{-4} M) acid with (-)-Riboflavin

FDCD titration of complex **1** and *R*(or *S*)-MetMan with additional aliquots of (-)-Riboflavin was performed to test the influence of this fluorescence interfering species on the FDCD output of the adduct *R*(or *S*)-MetMan•**1**. A solution containing complex **1** (10^{-5}) and *R*-MetMan (5×10^{-4} M) acid was prepared by dilution from the pure compounds in $\text{CH}_3\text{CN}/\text{H}_2\text{O}$ 3:1 with HEPES 20 mM (pH=7.4). The solution of (-)-Riboflavin was prepared by dilution within a solution 10^{-5} M of complex to a concentration of *R*-BINAPO equal to 2×10^{-3} M. A defined aliquot (-)-Riboflavin solution was then added to the solution containing complex **1** and *R*(or *S*)-MetMan to obtain a final concentration of (-)-Riboflavin equal to 5×10^{-4} M. The FDCD output were recorded with a 1.0 cm cuvette path length within the range 250 – 350 nm. The HT(V) of the phototube detector was fixed to 550 for all the measurements. FDCD/DC, FDCD spectra (mdeg), and DC(V) response are reported in Figure S27.

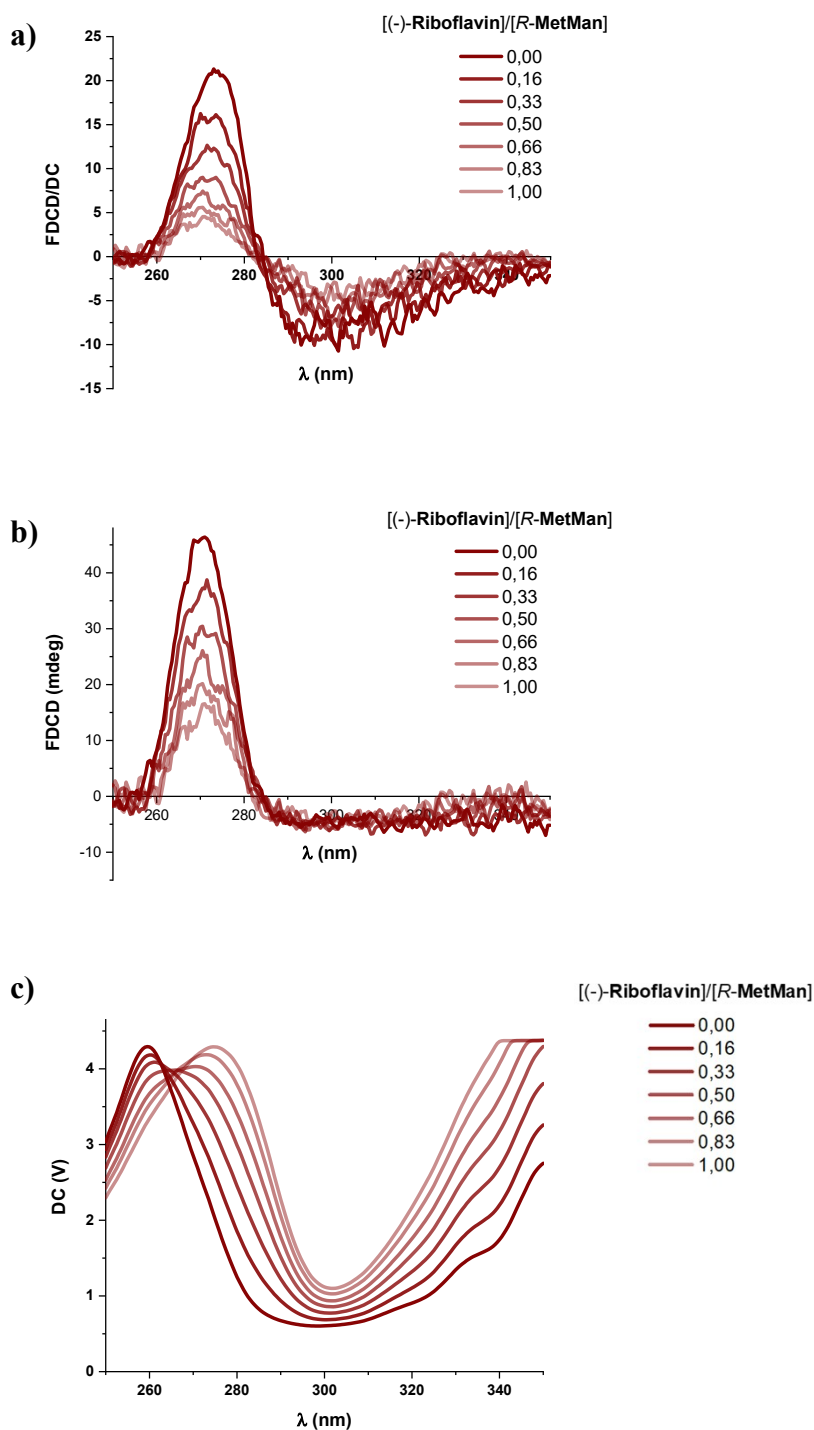


Figure S27. a) FDCD/DC, b) FDCD (mdeg), and c) DC (V) spectra for the titration of the host **1** (10^{-5} M) and *R*-MetMan acid (5×10^{-4} M) with additional aliquots of (-)-Riboflavin (from 0 M (solid line) to 5×10^{-4} M (faded line)).

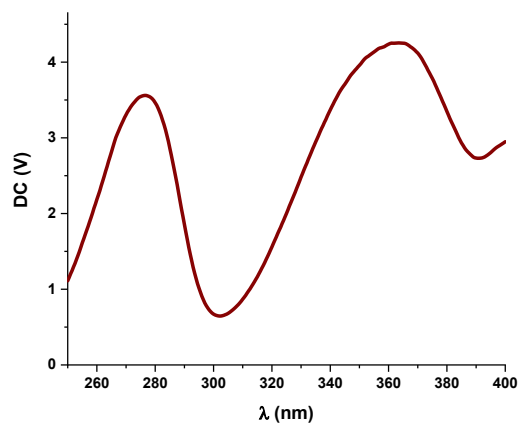
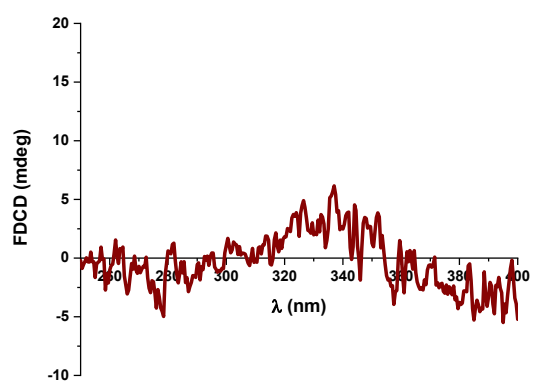
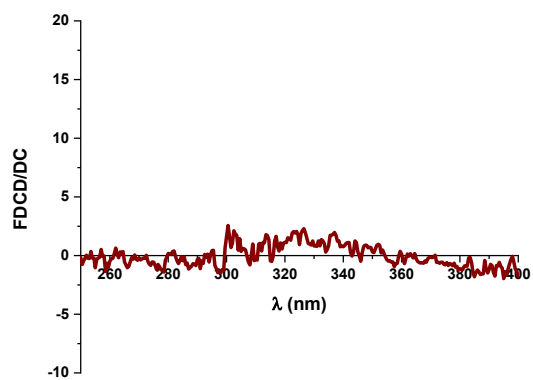


Figure S28. a) FDCD/DC, b) FDCD (mdeg), and c) DC(V) spectra of the “chiroptical contaminant” (-)-**Riboflavin** at a concentration equal to 5×10^{-4} M.

9. X-Ray measurements

9.1 Refinement Data for the species *R*-MetMan·1

Bond precision: C-C = 0.0100 Å Wavelength= 0.71073 nm

Cell: a= 11.0621 (6) b= 13.6834 (7) c= 15.7489 (8)
α= 77.7324 (8) β= 71.3068 (14) γ= 68.6923 (13)

Temperature: 183 K

	Calculated	Reported
Volume	2091.27 (19)	2091.27 (19)
Space group	P 1	P 1
Hall group	P 1	P 1
Sum formula	C ₈₈ H ₈₆ Cl ₃ N ₉ O ₁₈ Zn ₂	C ₈₈ H ₈₆ Cl ₃ N ₉ O ₁₈ Zn ₂
Mr	1794.79	1794.74
Dx, g cm ⁻³	1.425	1.425
Z	1	1
Mu (mm ⁻¹)	0.745	0.745
F000	932.0	932.0
F000'	933.39	
h, k, l _{max}	13,16,19	13,16,19
Nref	15586 [7793]	34921
T _{min} , T _{max}	0.844, 0.963	0.682, 0.887
T _{min} '	0.753	
Reported T Limits:	T _{min} = 0.682	T _{max} = 0.887
AbsCorr = MULTI-SCAN		
Data completeness= 4.48/2.24		θ (max)= 25.507
R(reflections)= 0.0418 (32708)		wR2(reflections)= 0.1007 (34921)
S = 1.034		Npar= 1091

9.2 Coordinates of the Atoms within the Unit Cell

Zn	5.43935	3.71906	3.3761
O	7.39307	3.45254	3.29958
O	7.73342	4.59852	5.1859
O	10.38511	3.84486	5.13696
N	3.34339	4.39922	3.69108
N	4.48613	2.88465	1.72171
N	5.55402	5.82316	3.2017
N	4.95157	2.72667	5.12361
C	2.75692	4.47466	2.36531
H	2.97298	5.35347	1.96195
H	12.83432	4.4074	2.43798
C	3.26791	3.37127	1.46219
C	2.49886	2.92632	4.02E-08
H	1.62241	3.26386	2.60E-08
C	8.0886	3.5948	14.38319
H	7.59473	3.28814	13.63133
C	9.35304	3.09223	14.63678
H	9.73819	2.4473	14.05546
C	5.00566	1.91451	9.18E-08
C	6.3223	1.35086	1.30055
C	7.47582	1.66429	5.77E-08
C	12.51633	4.11415	14.23638
H	11.6898	4.46649	13.92644
C	13.64178	4.40505	13.56312
H	13.59468	4.94146	12.78012
C	14.90197	3.918	14.00504
H	15.6937	4.13871	13.52901
C	9.91875	1.51677	2.77E-08
H	10.76191	1.19628	5.75E-08
C	8.73973	1.1686	9.98E-08
C	8.80432	3.39E-08	2.13101
H	14.62138	12.776	2.43353
C	12.63177	12.71318	2.81465
C	12.69677	11.77455	3.90611
H	13.53729	11.4274	4.18194
C	11.56513	11.38604	4.53785
H	11.61904	10.75467	5.24522
C	10.3113	11.89745	4.16711
H	9.53126	11.61935	4.63127
C	10.20978	12.79589	3.13942
H	4.38316	3.86E-08	2.89918
C	6.39167	4.82E-08	2.42315
C	14.47573	5.72854	4.34061
H	14.55582	5.61401	5.32085
H	13.64514	6.23347	4.15524
C	4.58638	6.49097	3.82899
C	4.6903	7.87808	4.05144
H	15.07017	8.34257	4.52153
C	5.788	8.54689	3.58134
H	5.86931	9.48335	3.71629
C	6.77549	7.85558	2.91401

H	7.53919	8.31097	2.57886
C	6.6391	6.48402	2.7405
H	7.32164	6.00108	2.2882
C	2.69111	3.4034	4.55119
H	2.30911	2.68281	3.98915
H	13.01044	3.83241	5.0465
C	3.67882	2.80526	5.53884
C	3.27661	2.30607	6.76673
H	13.4323	2.37977	7.04404
C	4.21034	1.70025	7.57939
H	3.95661	1.35982	8.42912
C	5.53147	1.59023	7.14488
H	6.19097	1.16855	7.6832
C	5.84798	2.11475	5.91551
H	6.74469	2.04052	5.61002
C	8.13446	3.97207	4.2027
C	9.64403	3.80265	3.94763
H	9.80185	2.92452	3.49533
C	10.08406	4.92406	3.02375
C	10.67936	6.06661	3.50423
H	10.85568	6.16184	4.43256
C	11.02023	7.08642	2.60704
H	11.4101	7.88861	2.93625
C	10.80173	6.94525	1.25903
H	11.05024	7.63802	6.58E-08
C	10.21747	5.78678	7.84E-08
H	15.12092	7.30029	14.68275
C	9.84518	4.79131	1.65943
H	9.42184	4.00825	1.33021
C	10.26868	2.62761	5.87251
H	10.50045	1.87193	5.29267
H	9.34621	2.52467	6.18986
H	10.87696	2.64906	6.63919
Zn	16.0933	10.18693	11.36063
O	18.02923	10.45771	11.51219
O	7.29569	9.20826	9.68222
O	9.97901	9.86993	9.70595
N	13.98875	9.54438	11.06434
N	15.15482	11.02645	13.03963
N	16.15534	8.06243	11.54778
N	15.60428	11.12264	9.57396
C	13.40619	9.44859	12.41382
H	13.62758	8.56593	12.80533
H	12.42035	9.51715	12.35302
C	13.93275	10.54496	13.31101
C	13.19592	10.98231	14.39505
H	12.3243	10.64018	14.55373
C	8.69747	10.29997	4.15E-08
H	8.21991	10.60393	1.17747
C	9.94436	10.78095	1.28E-08
H	10.34114	11.41585	7.10E-08
C	15.68491	11.98989	13.84043
C	16.98623	12.57788	13.43558

C	18.16058	12.31771	14.18003
C	13.1111	9.90504	5.46E-08
H	12.30242	9.51125	8.50E-08
C	14.258	9.71793	1.24717
H	14.23571	9.21184	2.05093
C	4.42552	10.2644	8.01E-08
H	5.21841	10.11657	1.30204
C	9.51807	12.60727	14.50776
H	10.34836	12.96571	14.21858
C	19.40132	12.85017	13.73366
C	19.44185	13.62249	12.5903
H	9.21883	13.93594	12.27443
C	18.28536	13.95461	11.88589
C	13.35331	2.09432	10.77219
H	14.18764	2.44671	10.48598
C	12.21178	2.44899	10.11079
H	12.24919	3.03933	9.36635
C	10.97319	1.92432	10.54678
H	10.178	2.18205	10.09448
C	15.86053	13.81506	11.5893
H	15.01314	13.46659	11.8414
C	17.02445	13.42546	12.31595
C	14.04263	8.24224	10.38366
H	14.16971	8.38197	9.41232
H	13.18705	7.76478	10.51712
C	15.17701	7.40673	10.92642
C	15.23636	6.04908	10.6936
H	14.52664	5.60249	10.24723
C	16.34235	5.35612	11.11772
H	5.34861	4.42325	10.9457
C	6.28986	6.00984	11.79098
H	7.04754	5.53945	12.11723
C	17.22274	7.36469	11.97487
H	6.85732	7.82945	12.42421
C	13.34696	10.57819	10.23685
H	13.04542	11.32684	10.81075
H	12.55276	10.19691	9.78158
C	14.33016	11.08287	9.21064
C	13.92025	11.53739	7.95902
H	13.00391	11.50359	7.70841
C	14.86796	12.03474	7.08705
H	14.61206	12.33801	6.22397
C	16.17885	12.09112	7.4741
H	16.84615	12.4407	6.89426
C	16.50656	11.62611	8.73461
H	17.41406	11.66793	9.01192
C	7.69973	9.87544	10.62983
C	9.20804	10.05712	10.88045
H	9.37787	10.96966	11.25119
C	9.62714	9.01539	11.89182
C	9.40718	9.25027	13.24576
H	9.01619	10.07083	13.52159
C	9.7493	8.30433	14.18892

H	4.53444	6.84833	2.80E-08
C	10.33611	7.11432	13.79891
H	10.59512	6.47152	14.44844
C	10.54074	6.86911	12.45535
H	10.9203	6.04249	12.18248
C	10.19901	7.81375	11.50032
H	10.35673	7.6379	10.58089
C	9.82372	10.93811	8.77317
H	10.36544	10.75661	7.97682
H	10.11734	11.77616	9.18543
H	8.88014	11.01201	8.51662
Cl	6.38758	12.4713	3.6761
O	1.18784	8.25E-08	2.80575
O	7.14217	12.92399	4.81071
O	16.20572	11.90718	4.09296
O	7.13907	11.43975	3.02523
Cl	7.07903	1.76849	10.80719
O	12.18425	13.73891	12.00008
O	7.75802	1.10304	9.75192
O	5.71749	1.99422	10.44001
O	7.69814	3.03984	11.05989
Cl	12.81763	7.8088	6.84162
O	12.56757	6.48619	7.02328
O	12.47771	8.14309	5.49435
O	14.1892	8.03684	7.02773
O	12.04802	8.59345	7.74548
N	8.01172	6.3863	7.35694
H	8.07308	5.75799	6.71779
C	8.93395	7.51559	7.18047
H	9.86141	7.17069	7.15081
H	8.86152	8.11408	7.96644
C	8.6741	8.314	5.93776
H	8.54158	7.70457	5.17997
H	9.43953	8.89718	5.75684
H	7.86962	8.85923	6.06232
C	6.57512	6.76068	7.46965
H	6.45224	7.26114	8.31493
H	6.35799	7.37796	6.72669
C	5.61276	5.66431	7.44592
H	5.74784	5.12712	6.63771
H	4.70236	6.02906	7.44741
H	5.73934	5.10083	8.23782
C	9.75508	5.11459	8.6664
H	10.37075	5.87734	8.63525
H	9.90091	4.54319	7.88339
H	9.91649	4.59849	9.4835
C	8.3614	5.60618	8.66195
H	8.22512	6.20147	9.44198
H	7.74587	4.83766	8.75686

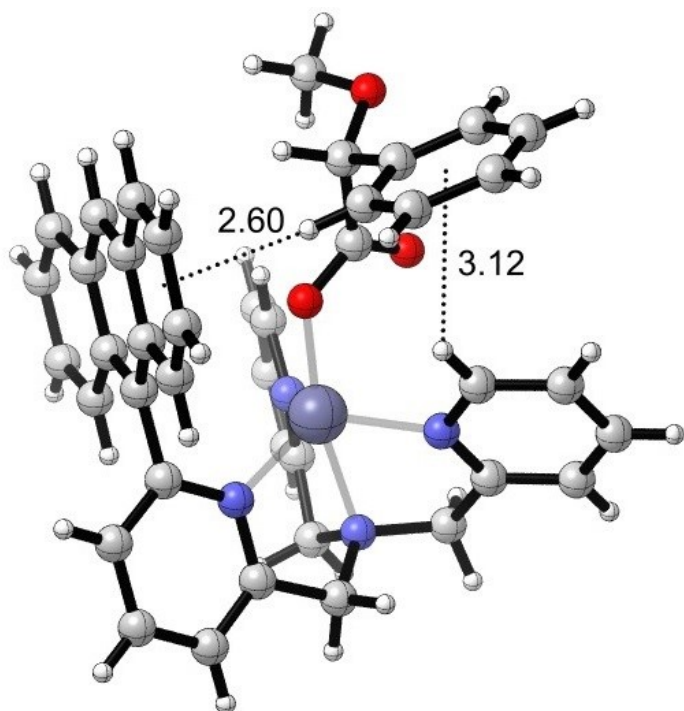


Figure S29. X-ray crystallographic structure of the complex *R-MetMan*·**1** between (*R*)-(-)-Methoxyphenylacetic *R-MetMan* acid and the stereodynamic probe based on Zn(II)-TPMA **1**.

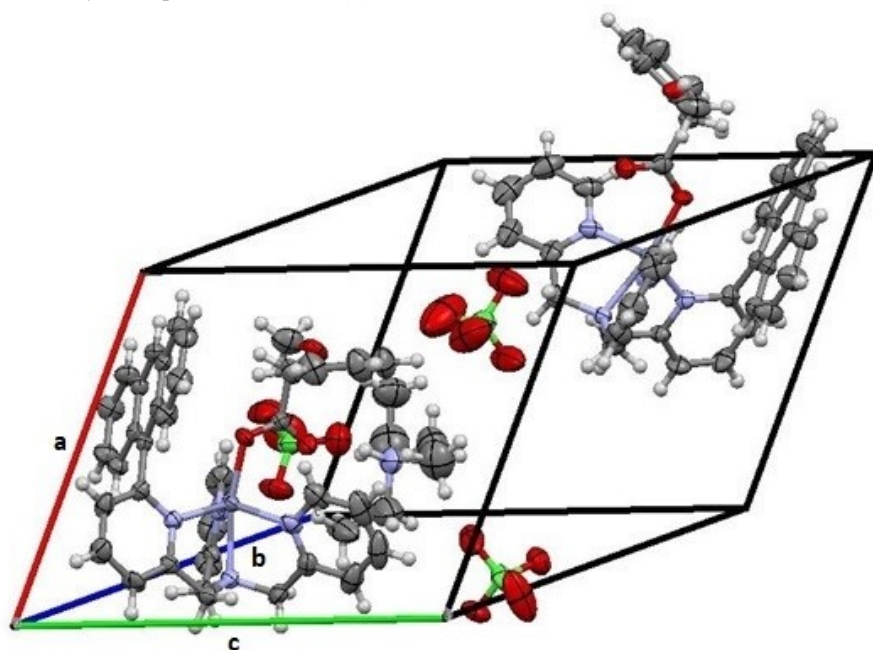


Figure S30. 3-D Crystal packing of *R-MetMan*·**1** molecule. One unit cell with two molecules of complex *R-MetMan*·**1** is displayed. Unit cell parameters are: space group P1, volume (\AA^3): 2091.27(19); a(\AA): 11.0621 (6), b(\AA): 13.6834(7), c(\AA): 15.7489(8); α ($^\circ$)= 77.7324 (8), β ($^\circ$)= 71.3068 $^\circ$ (14), γ ($^\circ$)= 68.6923 (13). Ellipsoids at the 50 % probability level are used.

10.DFT Calculation

Geometry of (*R*)-MetMan•1 complex has been optimized at M06/6-311+g(d,p) level starting from the X-ray structure obtaining conformer **A**. Other possible orientations of the (*R*)-metoxymandelic carboxylate within the host **1** have been considered, thus obtaining two other stable structures, one with a different orientation of the OCH₃ group (**B**), another one with the phenyl group pointing in opposite direction with respect to the former cases and with even higher energy (**C**), see *Figure S31*. Conformers **A**, **B** and **C** have Boltzmann populations of 77%, 19% and 4% respectively. The first two structures give quite similar calculated ECD spectra, while the lowest energy features of case **C** (consisting of three spectral components) have opposite sign with respect to **A** and **B** (see *Figure S32*). The average spectrum weighted with the Boltzmann population of three conformers is reported in *Figure S33*. The calculated spectra, in particular for the most populated conformer **A**, have been analyzed in term of electronic transitions responsible of CD and absorption bands as reported in *Table S1* and *Figure S34*. Molecular orbitals associated to the first three transitions are reported in *Figure S35*.

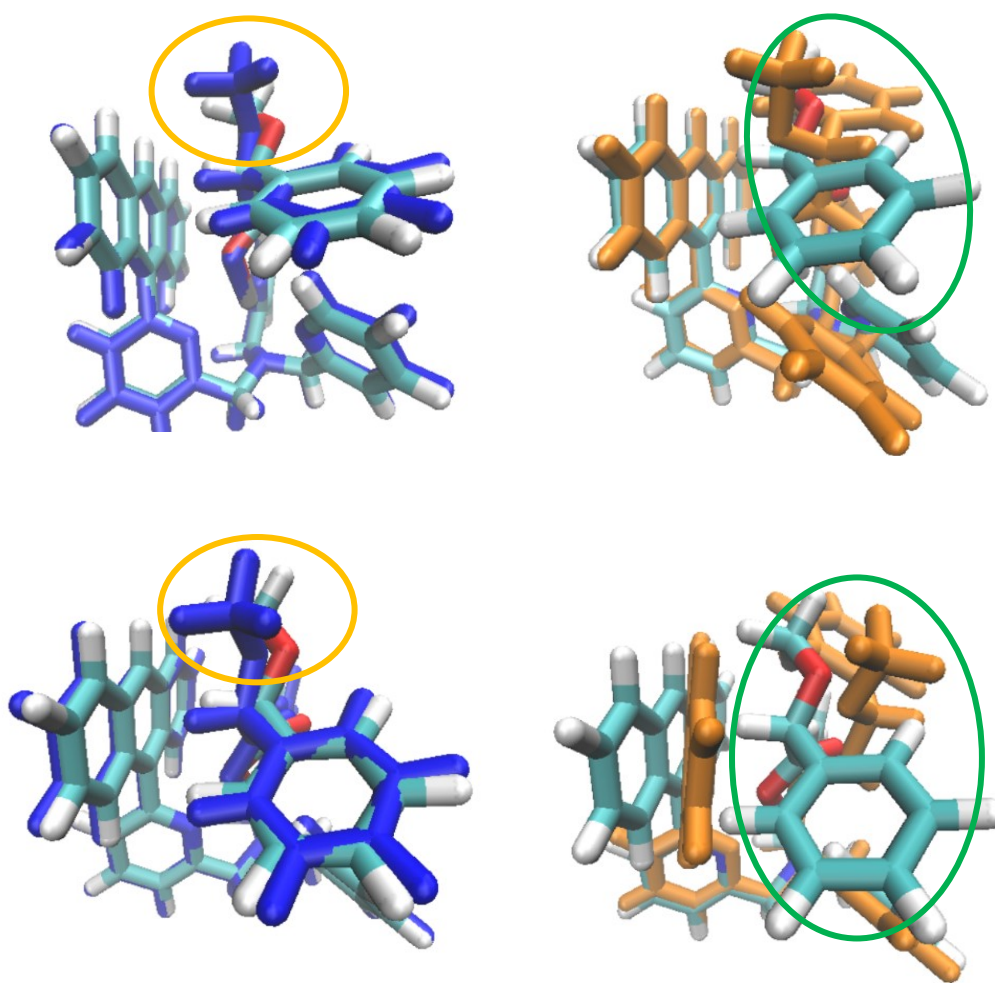


Figure S31. Host **1** and guests (*R*)-MetMan: superposition of structures **A**, **B** and **C**. Top left, structures **A** and **B** (blue); top right, structures **A** and **C** (orange) aligning the anthryl moiety. Bottom left, structures **A** and **B** (blue); bottom right, structures **A** and **C** (orange), as seen by aligning the N atoms of the tris(2-pyridylmethyl)amine.^[2]

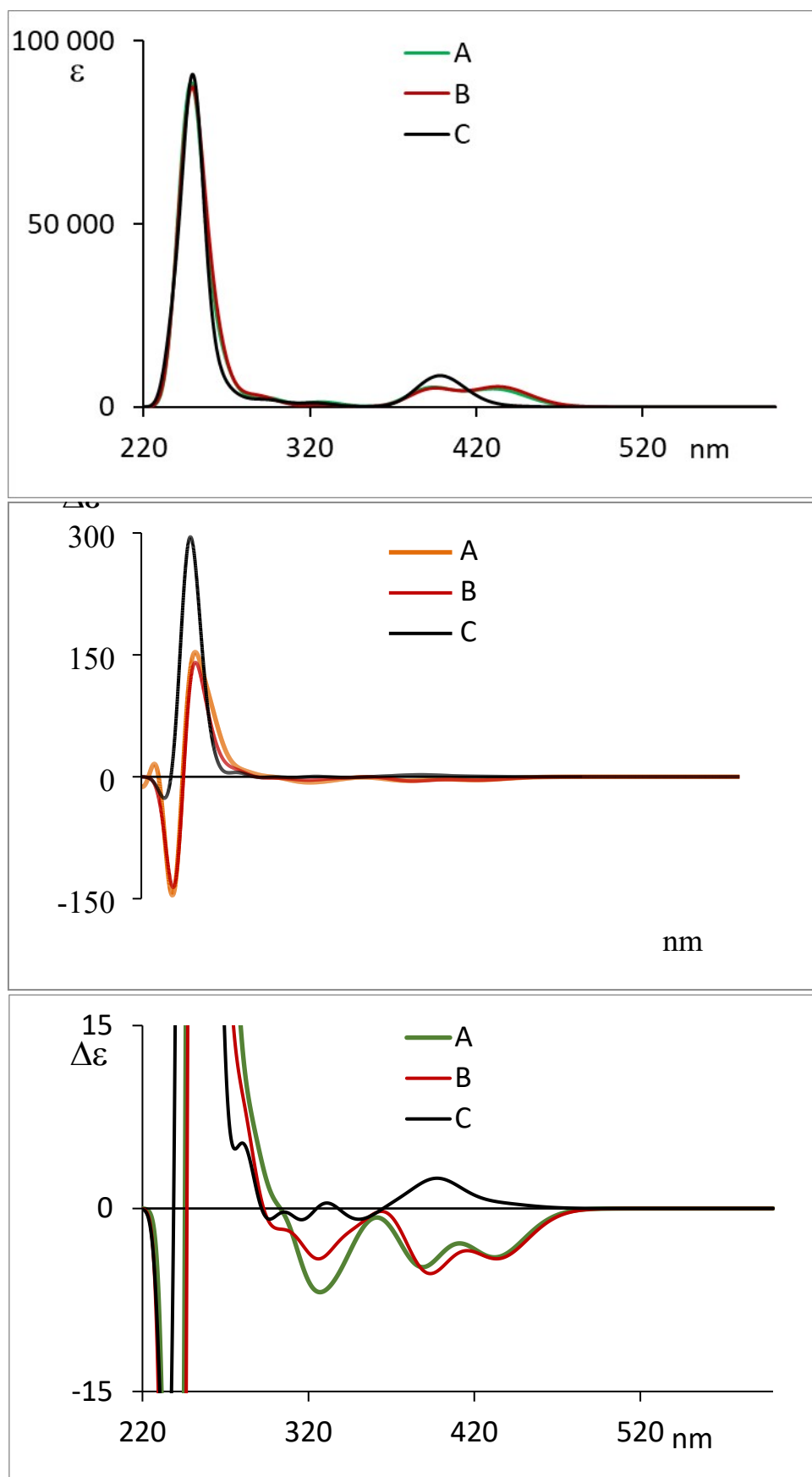


Figure S32. Calculated absorption and CD spectra of the three populated conformer of host **1** and guests (**R**)-MetMan, with 0.16 eV Gaussian bandwidth (calculated at M06/6-311+g(d,p) level).

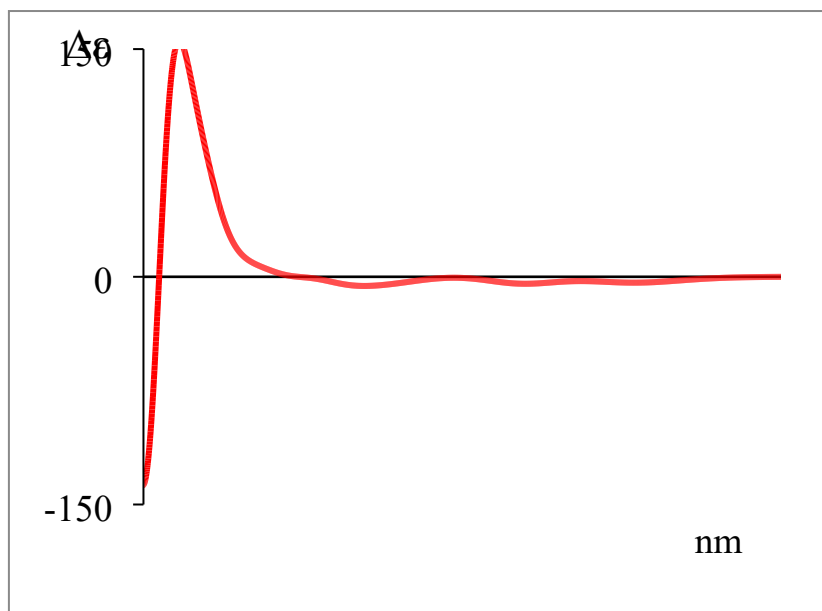


Figure S33. Calculated CD spectrum of *R*-MetMan hosted in **1** as Boltzmann weighed average of three most populated conformers.

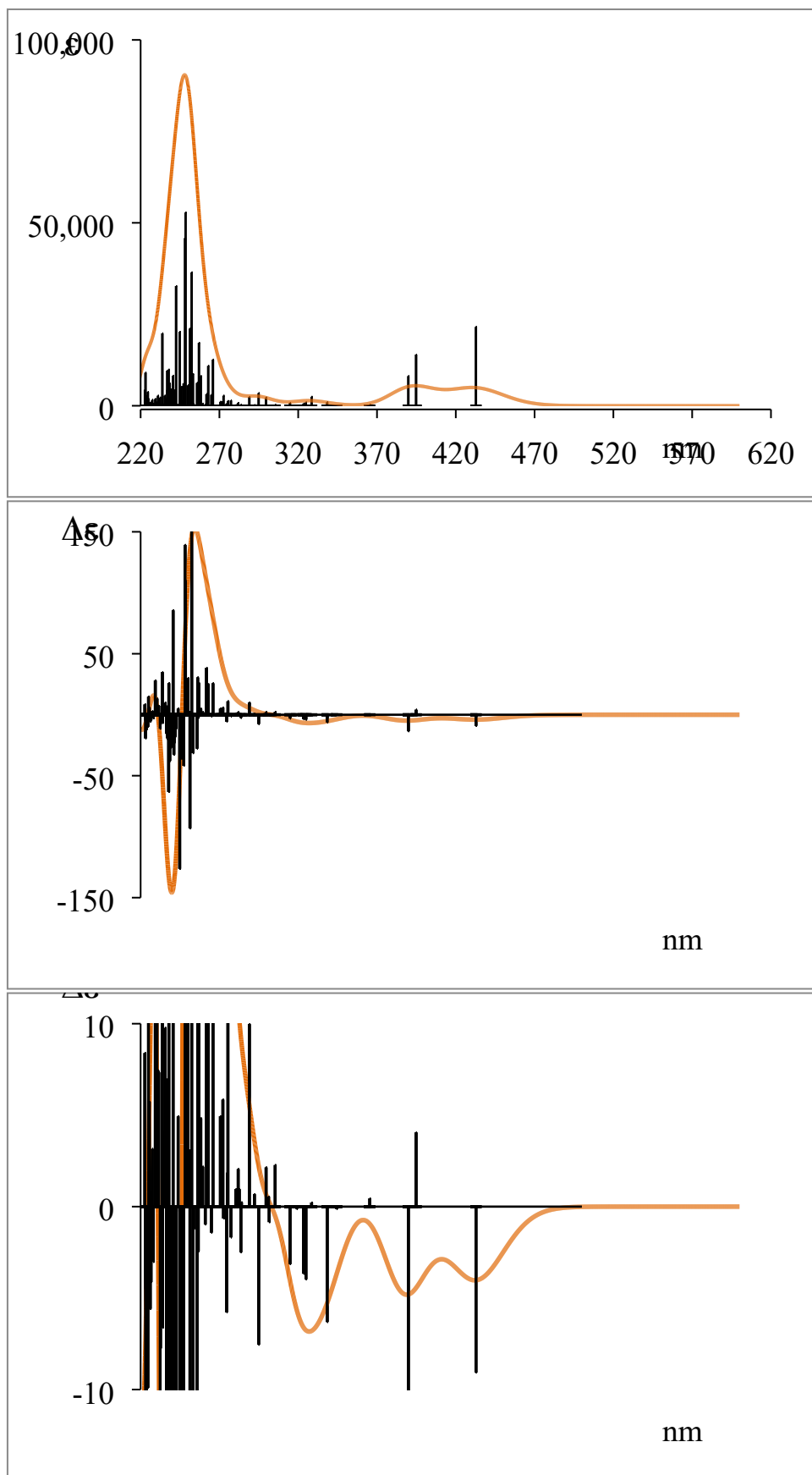
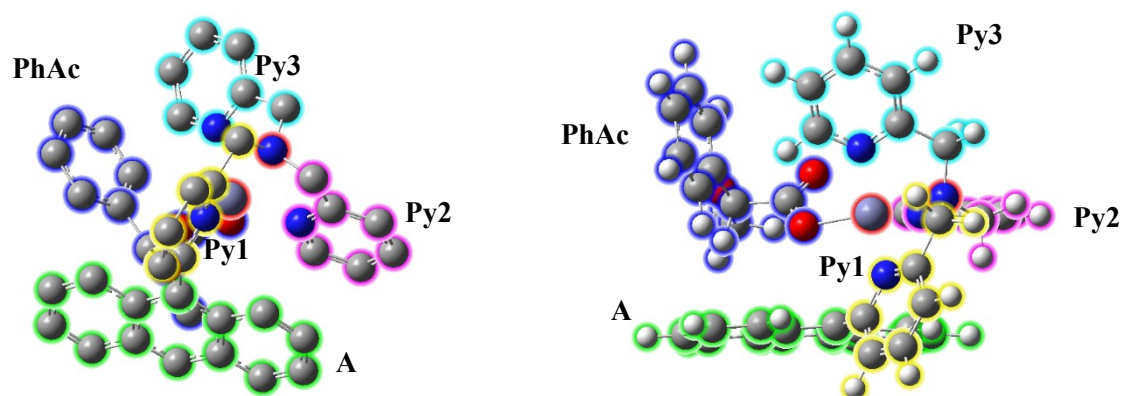


Figure S34. Calculated absorption and CD spectra of conformer A of host **1** and guests (*R*)-MetMan.

Table S1. Characteristics of the main transitions for the complex host **1** and guests (**R**)-MetMan:

Transition energy (eV) and wavelength (nm), dipole and rotational strength (10^{-40} esu²cm²), angle between electric and magnetic dipole transition moments (E-M in degrees), transition assignment, for each orbital the principal moiety contribution is given, moieties are defined in the figure below.

	eV	nm	D	R	E-M			
1	2.87	433	40221	-9.03	94	181(A) → 182(Py1,A)	0.68	
2	3.14	395	23848	4.07	87	181(A) → 183(Py2)	0.50	181(A) → 184(A,Py1,Py3) -0.44
3	3.18	390	14179	-13.52	103	181(A) → 183(Py2)	0.47	181(A) → 184(A,Py1,Py3) 0.49
6	3.66	338	2015	-6.31	126	180(PhAc) → 182(Py1,A)	0.67	
16	4.20	295	6460	-7.54	97	179(PhAc) → 185(Py3)	0.56	179(PhAc) → 184(A,Py1) -0.38
18	4.29	289	4672	9.98	76	178(A) → 183(Py2)	0.64	
25	4.50	275	2519	11.00	53	181(A) → 191(Py1)	0.60	
33	4.66	266	24486	25.75	81	176(PhAc,A) → 184(A,Py1)	0.46	176(PhAc,A) → 183(Py2) -0.32
35	4.72	263	21248	24.87	77	178(A) → 186(Py1)	0.46	176(PhAc,A) → 185(Py3) 0.29
46	4.91	252	70650	169.75	69	173(PhAc) → 182(Py1,A)	0.24	178(A) → 186(Py1) 0.20
48	4.93	251	41799	-93.16	109	173(PhAc) → 182(Py1,A)	0.47	178(A) → 187(Py2) -0.22
49	4.96	250	10738	30.10	60	181(A) → 196(A,Pyx)	0.49	178(A) → 187(Py2) 0.25
50	4.99	248	103526	109.78	81	178(A) → 187(Py2)	-0.32	177(PhAc) → 186(Py1) 0.33
51	5.00	248	89477	139.09	78	177(PhAc) → 186(Py1)	0.48	
52	5.01	247	12413	-41.98	117	174 → 183(Py2)	0.54	
54	5.04	246	10252	-36.27	104	181(A) → 198	0.28	179(PhAc) → 187(Py2) 0.27
55	5.05	246	3239	-12.21	134	181(A) → 198	0.39	175(A,PhAc) → 185(Py3) 0.24
56	5.06	245	39157	-126.26	112	171 → 182(Py1,A)	0.34	175(A,PhAc) → 185(Py3) 0.28



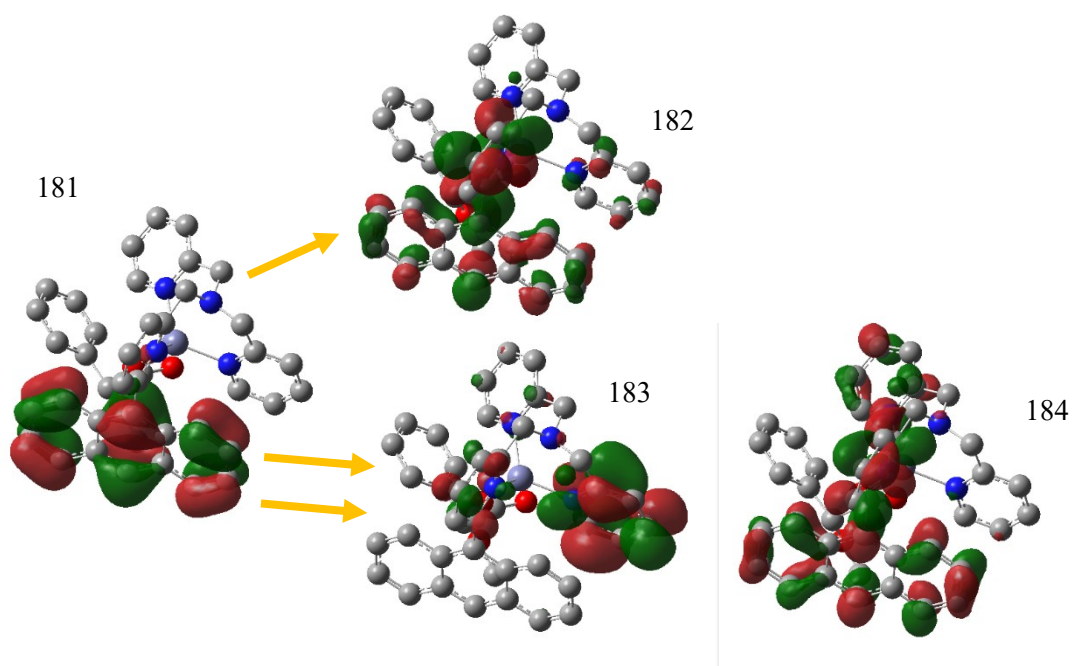


Figure S35. Molecular orbitals associated to the first three transitions (same orbital numbering as used in the *Table S1* above).

11. References

- [1] M. J. Frisch , G. W. Trucks , H. B. Schlegel , G. E. Scuseria , M. A. Robb , J. R. Cheeseman , G. Scalmani, V. Barone , G. A. Petersson , H. Nakatsuji , X. Li , M. Caricato , A. V. Marenich , J. Bloino , B. G. Janesko , R. Gomperts , B. Mennucci , H. P. Hratchian , J. V. Ortiz , A. F. Izmaylov , J. L. Sonnenberg , D. Williams-Young , F. Ding , F. Lipparini , F. Egidi , J. Goings , B. Peng , A. Petrone , T. Henderson , D. Ranasinghe , V. G. Zakrzewski , J. Gao , N. Rega , G. Zheng , W. Liang , M. Hada , M. Ehara , K. Toyota , R. Fukuda , J. Hasegawa , M. Ishida , T. Nakajima , Y. Honda , O. Kitao , H. Nakai , T. Vreven , K. Throssell , J. A. Montgomery, Jr. , J. E. Peralta , F. Ogliaro , M. J. Bearpark , J. J. Heyd , E. N. Brothers , K. N. Kudin , V. N. Staroverov , T. A. Keith , R. Kobayashi , J. Normand , K. Raghavachari , A. P. Rendell , J. C. Burant , S. S. Iyengar , J. Tomasi , M. Cossi , J. M. Millam , M. Klene , C. Adamo , R. Cammi , J. W. Ochterski , R. L. Martin , K. Morokuma , O. Farkas , J. B. Foresman and D. J. Fox , Gaussian 16, Revision C.01 , Gaussian, Inc., Wallingford CT, 2016